

1 **Exploring the impacts of unprecedented climate extremes on forest ecosystems: hypotheses**  
2 **to guide modeling and experimental studies**

3

4 Jennifer A. Holm<sup>1,\*</sup>, David M. Medvigy<sup>2</sup>, Benjamin Smith<sup>3,4</sup>, Jeffrey S. Dukes<sup>5,6</sup>, Claus Beier<sup>7</sup>,  
5 Mikhail Mishurov<sup>3</sup>, Xiangtao Xu<sup>8</sup>, Jeremy W. Lichstein<sup>9</sup>, Craig D. Allen<sup>10</sup>, Klaus S. Larsen<sup>7</sup>,  
6 Yiqi Luo<sup>11</sup>, Cari Ficken<sup>12</sup>, William T. Pockman<sup>13</sup>, William R.L. Anderegg<sup>14</sup>, and Anja Rammig<sup>15</sup>

7

8 <sup>1</sup> Lawrence Berkeley National Laboratory, Berkeley, California, USA

9 <sup>2</sup> University of Notre Dame, Notre Dame, Indiana, USA

10 <sup>3</sup> Dept of Physical Geography and Ecosystem Science, Lund University, Lund, Sweden

11 <sup>4</sup> Hawkesbury Institute for the Environment, Western Sydney University, Penrith, NSW 2751,  
12 Australia

13 <sup>5</sup> Department of Forestry and Natural Resources and Biological Sciences, Purdue University,  
14 West Lafayette, Indiana, USA

15 <sup>6</sup> Department of Global Ecology, Carnegie Institution for Science, Stanford, California, USA

16 <sup>7</sup> Department of Geosciences and Natural Resource Management, University of Copenhagen,  
17 Frederiksberg, Denmark

18 <sup>8</sup> Department of Ecology and Evolutionary Biology, Cornell University, Ithaca, New York, USA

19 <sup>9</sup> Department of Biology, University of Florida, Gainesville, Florida, USA

20 <sup>10</sup> Geography and Environmental Studies, University of New Mexico, Albuquerque, New  
21 Mexico, USA

22 <sup>11</sup> Center for Ecosystem Science and Society, Department of Biological Sciences, Northern  
23 Arizona University, Flagstaff, Arizona, USA

24 <sup>12</sup> Department of Biology, University of Waterloo, Waterloo, Ontario, Canada

25 <sup>13</sup> Department of Biology, University of New Mexico, Albuquerque, New Mexico, USA

26 <sup>14</sup> School of Biological Sciences, University of Utah, Salt Lake City, Utah, USA

27 <sup>15</sup> Technical University of Munich, TUM School of Life Sciences Weihenstephan, Freising,  
28 Germany

29

30 \* *Correspondence to:* Jennifer Holm; 510-495-8083; [jaholm@lbl.gov](mailto:jaholm@lbl.gov)

31

32 **Keywords:** demographic modeling; mortality; drought; recovery; carbon cycle; nonstructural  
33 carbohydrate storage; plant hydraulics; dynamic vegetation

34

35 **Abstract**

36

37 Climatic extreme events are expected to occur more frequently in the future, increasing the  
38 likelihood of unprecedented climate extremes (UCEs), or record-breaking events. UCEs, such as  
39 extreme heatwaves and droughts, substantially affect ecosystem stability and carbon cycling by  
40 increasing plant mortality and delaying ecosystem recovery. Quantitative knowledge of such  
41 effects is limited due to the paucity of experiments focusing on extreme climatic events beyond  
42 the range of historical experience. Here, we present a road map of how dynamic vegetation  
43 demographic models (VDMs) can be used to investigate hypotheses surrounding ecosystem  
44 responses to one type of UCE: unprecedented droughts. As a result of nonlinear ecosystem  
45 responses to UCEs, that are qualitatively different from responses to milder extremes, we  
46 consider both biomass loss and recovery rates over time, by reporting a time-integrated carbon  
47 loss as a result of UCE, relative to the absence of drought. Additionally, we explore how  
48 unprecedented droughts in combination with increasing atmospheric CO<sub>2</sub> and/or temperature  
49 may affect ecosystem stability and carbon cycling. We explored these questions using  
50 simulations of pre-drought and post-drought conditions at well-studied forest sites, using well-  
51 tested models (ED2 and LPJ-GUESS). The severity and patterns of biomass losses differed  
52 substantially between models. For example, biomass loss could be sensitive to either drought  
53 duration or drought intensity depending on the model approach. This is due to the models having  
54 different, but also plausible representations of processes and interactions, highlighting the  
55 complicated variability of UCE impacts still needed to be narrowed down in models. Elevated  
56 atmospheric CO<sub>2</sub> concentrations (eCO<sub>2</sub>) alone did not completely buffer the ecosystems from  
57 carbon losses during UCEs in the majority of our simulations. Our findings highlight the  
58 consequences of differences in process formulations and uncertainties in models, most notably  
59 related to availability in plant carbohydrate storage and the diversity of plant hydraulic schemes,  
60 in projecting potential ecosystem responses to UCEs. We provide a summary of the current state  
61 and role of many model processes that give way to different underlying hypotheses of plant  
62 responses to UCEs, reflecting knowledge gaps, which in future studies could be tested with  
63 targeted field experiments and an iterative modeling-experimental conceptual framework.

## 64 **1 Introduction**

65       The increase in extreme climate and weather events, such as prolonged heatwaves and  
66 droughts as seen over the last three decades, are expected to continue to increase in frequency  
67 and magnitude, leading to progressively longer and warmer droughts on land (IPCC 2012, 2021).  
68 Droughts are affecting all areas of the globe, more than any other natural disturbance, and recent  
69 droughts have broken long-standing records (Ciais et al., 2005; Phillips et al., 2009; Williams et  
70 al., 2012; Matusick et al., 2013; Griffin and Anchukaitis, 2014; Asner et al., 2016; Feldpausch et  
71 al., 2016; Seneviratne et al., 2021). Such ‘unprecedented climate extremes’ (UCEs; “record-  
72 breaking events”, IPCC (2012)) that are larger in extent and longer-lasting than historical norms  
73 can have dramatic consequences for terrestrial ecosystem processes, including carbon uptake and  
74 storage and other ecosystem services (Reichstein et al., 2013; Settele, 2014; Allen et al., 2015;  
75 Brando et al., 2019; Kannenberg et al., 2020). Thus, to better anticipate the implications of  
76 climatic changes for the terrestrial carbon sink and other ecosystem services, we need to better  
77 understand how ecosystems respond to extreme droughts and other UCEs.

78       To learn how ecosystems respond to rarely experienced or unprecedented conditions,  
79 ecologists can experimentally manipulate environmental conditions (Rustad, 2008; Beier et al.,  
80 2012; Meir et al., 2015; Aguirre et al., 2021). However, the majority of such experiments apply  
81 moderate treatments based on a historical sense, which are mostly weaker in intensity and/or  
82 shorter in duration than potential future UCEs (Beier et al., 2012; Kayler et al., 2015; but see Luo  
83 et al., 2017), and single experiments have low power to detect effects of stressors on ecosystem  
84 responses (Yang et al., 2022). Additionally, most experiments examine low-stature ecosystems,  
85 such as grassland, shrubland or tundra, due to lower requirements for infrastructure and financial  
86 investment compared to mature forests. However, forests may respond qualitatively differently  
87 to UCEs than other ecosystems, in part due to mortality of large trees and strong nonlinear  
88 ecosystem responses, with long-lasting consequences for ecosystem-climate feedbacks (Williams  
89 et al., 2014; Meir et al., 2015). Ecosystem responses to naturally occurring extreme droughts and  
90 heatwaves have been documented (Ciais et al., 2005; Breshears et al., 2009; Feldpausch et al.,  
91 2016; Matusick et al., 2016; Ruthrof et al., 2018; Powers et al., 2020); however, these rapidly-  
92 mobilized post-hoc studies often are unable to measure all critical variables and may lack  
93 consistently collected data for comparison with pre-drought conditions, thus limiting their  
94 inferential power and ability to improve quantitative models. The difficulties of performing

95 controlled real-world experiments of UCEs at broad spatial and temporal scales make process-  
96 based modeling a valuable tool for studying potential ecosystem responses to extreme events.

97         Process-based models can be used to explore potential ecosystem impacts using projected  
98 climate change over broad spatial and temporal scales (Gerten et al., 2008; Luo et al., 2008;  
99 Zscheischler et al., 2014; Sippel et al., 2016), as seen in a few modeling studies that have  
100 synthesized and improved our process-level understanding of UCE effects (McDowell et al.,  
101 2013; Dietze and Matthes, 2014). However, due to the overly simplified representation of  
102 ecological processes in most land surface models (LSMs) – the terrestrial components of Earth  
103 System Models (ESMs) used for climate projections – it is doubtful whether most of these  
104 models adequately capture ecosystem feedbacks and other responses to UCEs (Fisher and  
105 Koven, 2020). For example, only a few ESMs in recent coupled model intercomparison projects  
106 (CMIP6) (Arora et al., 2020; IPCC 2021) include vegetation demographics (Döscher et al.,  
107 2022), and most rely on prescribed, static maps of plant functional types (PFTs) (Ahlström et al.,  
108 2012). Other LSMs simulate PFT shifts (i.e., dynamic global vegetation models, DGVMs; Sitch  
109 et al., (2008)) based on bioclimatic limits, instead of emerging from the physiology- and  
110 competition-based demographic rates that determine resource competition and plant distributions  
111 in real ecosystems (Fisher et al., 2018). While a new generation of LSMs with more explicit  
112 ecological dynamics and structured demography is emerging (Holm et al., 2020; Koven et al.,  
113 2020; Döscher et al., 2022), most current ESMs are limited in ecological detail and realism (e.g.,  
114 ecosystem structure, demography, and disturbances). Failing to mechanistically represent  
115 mortality, recruitment, and disturbance – each of which influences biomass turnover and carbon  
116 (C) allocation (Friend et al., 2014) – limits the ability of these models to realistically forecast  
117 ecosystem responses to anomalous environmental conditions like UCEs (Fisher et al., 2018).

118         Evaluating and improving the representation of physiological and ecological processes in  
119 ecosystem models is critical for reducing model uncertainties when projecting the effects of  
120 UCEs on long-term ecosystem dynamics and functioning. Vegetation demography, plant  
121 hydraulics, enhanced representations of plant trait variation, explicit treatments of resource  
122 competition (e.g., height-structured competition for light), and representing major disturbances  
123 (e.g., extreme drought) have all been identified as critical areas for advancing current models  
124 (Scheiter et al., 2013; Fisher et al., 2015; Weng et al., 2015; Choat et al., 2018; Fisher et al.,  
125 2018; Blyth et al., 2021) and are necessary advances for realistically representing the ecosystem

126 impacts of UCEs. In this perspectives focused paper we look at the differences in these  
127 processes, and how they contribute to uncertainty across multiple temporal phases surrounding  
128 an extreme event: predicting an ecosystem's pre-disturbance resistance, which influences the  
129 degree of impact and recovery from UCEs. Table 1 describes a summary of model mechanisms  
130 that affect pre-drought resistance and post-drought recovery and we suggest are critical areas  
131 further research (ca. Frank et al., 2015).

132 In order to inform our discussion, we explore the potential responses of forest ecosystems  
133 to UCEs using two state-of-the-art process-based demographic models (vegetation demographic  
134 models, VDMs; Fisher et al., (2018)), a unique model exploration-discussion approach to help  
135 highlight new paths forward for model advancement. We first present conceptual frameworks  
136 and hypotheses on potential ecosystem responses to UCEs based on current knowledge. We then  
137 present VDM simulations for a range of hypothetical UCE scenarios to illustrate current state-of-  
138 the-art model representations of eco-physiological mechanisms expected to drive responses to  
139 UCEs, using droughts as an example. While a variety of UCE-linked biophysical tree  
140 disturbance processes (e.g., fire, wind, insect outbreaks) can drive nonlinear ecosystem  
141 responses, we focus specifically on extreme droughts, which have important impacts on many  
142 ecosystems around the world (e.g. Frank et al., 2015, IPCC 2021). By studying modeled  
143 responses to UCEs, we explore the limits to our current understanding of ecosystem responses to  
144 extreme droughts and their corresponding thresholds and tipping points. As anthropogenic  
145 forcing has increased the frequency, duration, and intensity of droughts throughout the world  
146 (Chiang et al., 2021), we explore how eCO<sub>2</sub> and rising temperatures may affect drought-induced  
147 C loss and recovery trajectories. This study can help guide how the scientific community can  
148 iteratively address these questions through future experiments and modeling studies. We believe  
149 the combination of using cutting-edge VDMs alongside an inspection of current gaps in  
150 knowledge will help guide modeling and experimental advances in order to address novel forest  
151 responses to climate extremes.

152

### 153 **1.1 Conceptual and Modeling Framework for Hypothesis Testing:**

154 We combine conceptual frameworks (Fig. 1) and ecosystem modeling to test two  
155 hypotheses on potential responses of plant carbon stocks to UCEs. The first hypothesis is:

156 ***Hypothesis (H1). Terrestrial ecosystem responses to UCEs will differ qualitatively from***  
157 ***ecosystem responses to milder extremes because responses are nonlinear and highly variable.***  
158 ***Nonlinearities can arise from multiple mechanisms – including shifts in plant hydraulics, C***  
159 ***allocation, phenology, and stand demography – and can vary depending on the pre-drought***  
160 ***state of the ecosystem.***

161 We present three conceptual relationships that describe terrestrial ecosystem responses to  
162 varying degrees of extreme events (Fig. 1). We hypothesize that change in vegetation C stock is  
163 related to drought intensity and/or drought duration, such that biomass loss increases nonlinearly  
164 with increased drought intensity (i.e., reduction in precipitation) represented by a threshold-based  
165 relationship (Fig. 1a, H1a), increased drought duration (i.e., prolonged drought with the same  
166 intensity) by shifting responses typically seen in milder extremes downwards via increasing  
167 slopes (Fig. 1a, H1b), or the combination of both intensity and duration (Fig. 1a, H1c). These  
168 hypotheses are supported by observations from the Amazon Basin and Borneo (Phillips et al.,  
169 2010) where tree mortality rates increased nonlinearly with drought intensity. Similarly, plant  
170 hydraulic theories predict nonlinear damage to the plant-water transport systems, and thus  
171 mortality risk, as a function of drought stress (Sperry and Love, 2015). In particular, longer  
172 droughts are more likely to lead to lower soil water potentials, leading to a nonlinear xylem  
173 damage function even if stomata effectively limit water loss (Sperry et al., 2016).

174 ***Hypothesis (H2): The effects of increasing atmospheric CO<sub>2</sub> concentration (eCO<sub>2</sub>) will***  
175 ***alleviate impacts of extreme drought stress through an increase in vegetation productivity and***  
176 ***water-use efficiency, but only up to a threshold of drought severity, while increased***  
177 ***temperature (and related water stress) will exacerbate tree mortality.***

178 This second hypothesis is based on growing evidence that effects of eCO<sub>2</sub> and climate  
179 warming may interact with effects of drought intensity on ecosystems. The CO<sub>2</sub> fertilization  
180 effect enhances vegetation productivity (e.g., net primary production, NPP) (Ainsworth and  
181 Long, 2005; Norby et al., 2005; Wang et al., 2012), but this fertilization effect is generally  
182 reduced by drought (Hovenden et al., 2014; Reich et al., 2014; Gray et al., 2016). Drought events  
183 often coincide with increased temperature, which intensifies the impact of drought on  
184 ecosystems (Allen et al., 2015; Liu et al., 2017), resulting in nonlinear responses in mortality  
185 rates (Adams et al., 2009; Adams et al., 2017a). The evaluation of C cycling in VDMs with

186 doubling of CO<sub>2</sub> (only “beta effect”) showed a large carbon sink in a tropical forest (Holm et al.,  
187 2020), but the inclusion of climate interactions in VDMs needs to be further explored.

188 Here, we relate ecosystem responses to UCEs by calculating a “severity-drought index”  
189 (Fig. 1b and see Methods), which integrates C loss from the beginning of the drought until the  
190 time when C stocks have recovered to 50% of the pre-drought level. In response to drought,  
191 warming, and eCO<sub>2</sub>, divergent potential C responses (gains and losses; Fig. 1c) can be expected  
192 (Keenan et al., 2013; Zhu et al., 2016; Adams et al., 2017a). For example, a grassland  
193 macrocosm experiment found that eCO<sub>2</sub> completely compensated for the negative impact of  
194 extreme drought on net carbon uptake due to increased root growth and plant nitrogen uptake,  
195 and led to enhanced post-drought recovery (Roy et al., 2016). However, a 16-year grassland  
196 FACE and the SoyFACE experiments showed that CO<sub>2</sub> fertilization effects were reduced or  
197 eliminated under hotter/drier conditions (Gray et al., 2016; Obermeier et al., 2016). Reich et al.,  
198 (2014) also found that CO<sub>2</sub> fertilization effects were reduced in a perennial grassland by water  
199 and nitrogen limitation.

200 A corollary to our H2 is that conditions that favor productivity (e.g., longer growing  
201 seasons and/or CO<sub>2</sub> fertilization) will enhance vegetation growth leading to “structural  
202 overshoot” (SO; Fig. 1d; adapted from and supported by Jump et al., 2017), and can amplify the  
203 effects of UCEs. Enhanced vegetation growth coupled with environmental variability can lead to  
204 exceptionally high plant-water-demand during extreme drought and water stress, resulting in a  
205 “mortality overshoot” (MO; Fig 1d). We conceptualize how oscillations between SO and  
206 associated MO could be amplified by increasing climatic variability and UCEs (Fig. 1d).  
207 Additionally, more climatic variability from unprecedented eCO<sub>2</sub> levels and warming will  
208 contribute to unknowns in how ecosystems are affected in the future (i.e., the widening, and  
209 downward shape of the shaded areas compared to historical, Fig. 1d). We expect, however that a  
210 rapidly changing climate, combined with effects of UCEs as a result of more frequent extreme  
211 drought/heat events and drought stress, can exacerbate and amplify SOs and MOs (Jump et al.,  
212 2017), leading to increasing C loss, even though various buffering mechanisms exist (cf. (Lloret  
213 et al., 2012; Allen et al., 2015)). Relative to our conceptual (Fig. 1d), we note that most  
214 experimental, observational and modeling studies (Ciais et al., 2005; da Costa et al., 2010;  
215 Phillips et al., 2010; Meir et al., 2015) take into account only low to moderate drought intensities

216 (such as 50% rain excluded) or single events, or combine drought with moderate effects of  
217 temperature change. Where there has been 100% rain exclusion, it was on very small plots of 1.5  
218 m<sup>2</sup> (Meir et al., 2015). As represented by the increasing amplitude of oscillations in Fig. 1d, the  
219 interactions between increased temperatures, UCE events, and vegetation feedbacks make  
220 ecosystem states become inherently unpredictable, particularly over longer time-scales.

221

## 222 **2 Vegetation Demography Model (VDM) Approaches**

223 We argue that VDMs are well suited to address climate change impacts due to the  
224 inclusion of detailed process representation of dynamic plant growth, recruitment, and mortality,  
225 resulting in changes in abundance of different PFTs, as well as vertically stratified tree size- and  
226 age-class structured ecosystem demography. Community dynamics and age-/size-structure are  
227 emergent properties from competition for light, space, water, and nutrients, which dynamically  
228 and explicitly scale up from the tree, to stand, to ecosystem level. Within this characterization,  
229 VDMs also differ between each other and are set up in different configuration, allowing for  
230 various testing capabilities. For full names of each model listed below and references, see Table  
231 S1. For example, VDMs can aggregate and track the community level disturbance into either  
232 patch-tiling sampling (e.g., ED2, FATES, LM3-PPA, ORCHIDEE, JSBACH4.0) or statistical  
233 approximations (e.g., LPJ-GUESS, SEIB-DGVM, and CABLE-POP). VDMs could also vary in  
234 representing light competition within either multiple canopy layers (e.g., ED2, FATES, LM3-  
235 PPA, LPJ-GUESS, SEIB-DGVM) or in a single canopy (e.g., JSBACH4.0, ORCHIDEE,  
236 CABLE-POP).

237 Powell et al. (2013) compared multiple VDMs and LSMs to interpret ecosystem  
238 responses to long-term droughts in the Amazon and are informative when conducting model-data  
239 comparisons, but studies of the cascade of ecosystem responses and mortality to UCEs are  
240 lacking. In a cutting-edge area of development, new mechanistic implementation of plant  
241 competition for water and plant hydraulics in VDMs (i.e., hydrodynamics) are improving our  
242 understanding of plant-water relations and stresses within plants, such as with TFSv.1-Hydro  
243 (Christoffersen et al., 2016), ED2-hydro (Xu et al., 2016), and FATES-HYDRO (Ma et al., 2021;  
244 Fang et al., 2022). Compared to more simplistic representation of plant acquiring soil moisture  
245 not connected to plant physiology (e.g., LPJ-GUESS, LM3-PPA, CABLE-POP, SEIB-DGVM).



246 For hydrodynamic representations in ‘big-leaf’ LSMs such as CLM5, JULES, and Noah-MP-  
247 PHS see Kennedy et al., (2019), Eller et al., (2020), and Li et al., (2021) respectively.

248 The discussion section provides a deeper investigation of model response to UCEs related  
249 to droughts. An exhaustive review of all VDMs, and all plant processes is too large to be done  
250 here. Existing review papers of different VDM development, processes, and uncertainties can be  
251 found here: Fisher et al., (2018); Bonan (2019); Trugman et al., (2019); Hanbury-Brown et al.  
252 (2022); Bugmann and Seidl (2022); and specifically related to plant hydraulics see: Mencuccini  
253 et al., (2019); Anderegg and Venturas (2020). We use LPJ-GUESS and ED2 as example VDMs  
254 in an initial guide framework to explore hypotheses around vegetation mortality and severity  
255 index from UCEs and climate change impacts, and highlight limiting model processes. Since  
256 field data needed to evaluate UCE responses are, by definition, unavailable, we do not perform  
257 model-data comparisons. Rather, we use the model results and conceptual framework as a road  
258 map to explore our hypotheses and illustrate their implications for ecosystem responses under  
259 UCEs, not historical drought events.

260

## 261 **2.1 LPJ-GUESS and ED2 Model Descriptions**

262 We explored our hypotheses at forested ecosystems in Australia and Central America  
263 using two VDMs: the Lund-Potsdam-Jena General Ecosystem Simulator (LPJ-GUESS) (Smith et  
264 al., 2001; Smith et al., 2014) and the Ecosystem Demography model 2 (ED2) (Medvigy et al.,  
265 2009; Medvigy and Moorcroft, 2012). Both LPJ-GUESS and ED2 resolve vegetation into tree  
266 cohorts characterized by their PFT, in addition to age-class in LPJ-GUESS; and size, and stem  
267 number density in ED2. Both models are driven by external environmental drivers (e.g.,  
268 temperature, precipitation, solar radiation, atmospheric CO<sub>2</sub> concentration, nitrogen deposition),  
269 and soil properties (soil texture, depth, etc.), and also depend on dynamic ecosystem state, which  
270 includes light attenuation, soil moisture, and soil nutrient availability. Establishment and growth  
271 of PFTs, and their carbon-, nitrogen- and water-cycles, are simulated across multiple patches per  
272 grid cell to account for landscape heterogeneity. Both models characterize PFTs by physiological  
273 and bioclimatic parameters, which vary between the models (Smith et al., 2001; Smith et al.,  
274 2014; Medvigy et al., 2009; Medvigy and Moorcroft, 2012).

275 The LPJ-GUESS includes three woody PFTs: evergreen, intermediate evergreen, and  
276 deciduous PFTs. Mortality in LPJ-GUESS is governed by a ‘growth-efficiency’-based function

277 (kg C m<sup>-2</sup> leaf yr<sup>-1</sup>), which captures effects of water deficit, shading, heat stress, and tree size on  
278 plant productivity relative to its resource-uptake capacity (leaf area), with a threshold below  
279 which stress-related mortality risk increases markedly, in addition to background senescence and  
280 exogenous disturbances. Stress mortality can be reduced by plants using labile carbon storage,  
281 modeled implicitly using a ‘C debt’ approach, which buffers low productivity, enhancing  
282 resilience to milder extremes (more details are given in section 4.1.4). Total mortality can thus be  
283 impacted by variation in environmental conditions such as water limitation, low light conditions,  
284 and nutrient constraints, as well as current stand structure (Smith et al., 2001; Hickler et al.,  
285 2004).

286         The ED2 version used here (Xu et al., 2016) includes four woody PFTs: evergreen,  
287 intermediate evergreen, deciduous, brevi-deciduous, and deciduous stem-succulent. This ED2  
288 version includes coupled photosynthesis, plant hydraulics, and soil hydraulic modules (Xu et al.,  
289 2016), which together determine plant water stress. The plant hydraulics module tracks water  
290 flow along a soil–plant–atmosphere continuum, connecting leaf water potential, stem sap flow,  
291 and transpiration, thus influencing controls on photosynthetic capacity, stomatal closure,  
292 phenology, and mortality. Leaf water potential depends on time-varying environmental  
293 conditions as well as time-invariant PFT traits. Leaf shedding is triggered when leaf water  
294 potential falls below the turgor loss point (a PFT trait) for a sufficient amount of time. Leaf  
295 flushing occurs when stem water potential remains high (above half of the turgor loss point) for a  
296 sufficient time (see Xu et al., 2016 for details). PFTs differ in their hydraulic traits, wood  
297 density, specific leaf area, allometries, rooting depth, and other traits. Stress-based mortality in  
298 the ED2 version used here includes two main physiological pathways in our current  
299 understanding of drought mortality (McDowell et al., 2013): C starvation and hydraulic failure.  
300 Mortality due to C starvation in ED2 results from a reduction of C storage, a proxy for non-  
301 structural carbohydrate (NSC) storage, which integrates the balance of photosynthetic gain and  
302 maintenance cost under different levels of light and moisture availability. Mortality due to  
303 hydraulic failure in ED2 is based on the percentage loss of stem conductivity. ED2 also includes  
304 a density-independent senescence mortality rate based on wood density.

## 305 **2.2 Modeling guide**

306 To exemplify how VDMs can be tools to explore new hypotheses related to UCEs we  
307 applied the models at two field sites, that were chosen due to being extensively studied and the  
308 models used here have already been run at these sites and previously benchmarked against field  
309 data (see Xu et al., 2016; Medlyn et al., 2016; Medvigy et al., 2019 for model-data validation).  
310 The purpose of this paper was not to do a large multi-site comparison, but rather just select a few  
311 for hypothesis testing. In addition, the two sites span a range of vegetation types and are in  
312 warm, seasonally dry climates that are more likely to experience droughts in the future (Allen et  
313 al., 2017). The first is a mature *Eucalyptus* (*E. tereticornis*) warm temperate-subtropical  
314 transitional forest that is the site of the Eucalyptus Free Air CO<sub>2</sub> enrichment (EucFACE)  
315 experiment in Western Sydney, Australia (Medlyn et al., 2016; Ellsworth et al., 2017; Jiang et  
316 al., 2020). The second site is a seasonally dry tropical forest in the Parque Nacional Palo Verde  
317 in Costa Rica (Powers et al., 2009). Site description details can be found in Supplement Text A.

318 We performed a 100-year “baseline” simulation for each model at each site driven by  
319 constant, near ambient, atmospheric CO<sub>2</sub> (400 ppm) and recycled historical site-specific climate  
320 data (1992-2011 for EucFACE and 1970-2012 for Palo Verde; Sheffield et al., (2006)), absent of  
321 drought treatments. A detailed description of the meteorological data and initial conditions used  
322 to drive the models is in the Supplementary Text A. The two models were previously tuned for  
323 each site (Xu et al., 2016; Medlyn et al., 2016), and no additional site-level parameter tuning was  
324 conducted here due to evaluating responses from hypothetical UCEs. To describe the ecosystem  
325 impact of UCEs, we simulated 10 years of pre-drought conditions (continuing from the baseline  
326 simulation), followed by drought treatments that differed in intensity and duration, followed by a  
327 100-year post-drought recovery period. To explore the effects of drought intensity, we conducted  
328 20 different artificial drought intensity simulations, in which precipitation during the whole year  
329 is reduced by 5% to 100% of its original amount, in increments of 5%. To explore the effects of  
330 drought duration, the 20 different drought intensities are maintained over 1, 2 and 4 years (Table  
331 S2). We examined model responses of aboveground biomass, leaf area index (LAI), stem density  
332 (number ha<sup>-1</sup>), plant available soil water (mm), plant C storage (kg C m<sup>-2</sup>), change in stem  
333 mortality rate (yr<sup>-1</sup>), and PFT composition.

334 To explore how temperature, eCO<sub>2</sub> concentration, and UCE droughts influence forest C  
335 dynamics individually and in combination, we implemented the following five experimental  
336 scenarios, some realistic and others hypothetical, for each model (Table S2): increased

337 temperature only (+2K over ambient), eCO<sub>2</sub> only (600 ppm and 800 ppm), and both increased  
 338 temperature and eCO<sub>2</sub> (+2K 600 ppm; +2K 800 ppm). Temperature and eCO<sub>2</sub> manipulations  
 339 were applied as step increases over the baseline conditions, and are artificial scenarios, as  
 340 opposed to model-generated climate projections.

341

### 342 **2.3 Linking concepts, hypotheses, and model outcomes**

343 To relate our simulation results to Fig. 1a, we compared the total biomass loss as a result  
 344 of each drought treatment by calculating the percentage of biomass reduction at the end of the  
 345 drought period relative to the baseline (no drought) simulation. To explicitly consider biomass  
 346 recovery rates over time, we calculated “severity-drought index” (Eqs. 1-3), as a result of  
 347 drought under current climate, which are determined based on the concepts in Fig. 1b. We  
 348 defined “severity-drought index” as the time-integrated carbon in biomass that is lost due to  
 349 drought relative to what the vegetation would have stored in the absence of drought. That is, it is  
 350 the difference between biomass in the presence of drought ( $B_d$ ) at time ( $t$ ) and biomass in the  
 351 baseline simulation (no drought;  $B_{base}$ ), integrated over a defined recovery time period (in kg C  
 352 m<sup>-2</sup> yr):

$$\text{Severity-drought index} = \int_{t=t_1}^{t=t_2} (B_{base}(t) - B_d(t)) dt \quad (\text{Eq. 1})$$

353

354 To define the bounds of integration, in Eq. 1,  $t_1$  is defined as the time when the maximum  
 355 amount of plant C is lost as a result of the drought:

$$B_{base}(t_1) - B_d(t_1) = \max_t [B_{base}(t) - B_d(t)] \quad (\text{Eq. 2})$$

356

357 Then,  $t_2$  is defined implicitly as the time when 50% of the lost biomass has been recovered  
 358 compared to the baseline:

$$B_{base}(t_2) - B_d(t_2) = \frac{1}{2} (B_{base}(t_1) - B_d(t_1)) \quad (\text{Eq. 3})$$

359

360 Since all severity-drought index results are taken as the difference from a non-drought baseline  
 361 biomass ( $B_{base}$ ) and all droughts will result in a loss of C.

362 We also use the severity-drought index as a starting point to examine the role of drought,  
 363 temperature and eCO<sub>2</sub> change for moderating or exacerbating the impacts of drought on forest C

364 stocks; i.e., to evaluate the hypotheses illustrated in Fig. 1c. To assess these impacts of changing  
365 climates, we calculate a severity-climate index (Eq. 4). Defined as the difference between the  
366 severity-drought index due to drought alone (Eqs. 1-3) under present climate, and the severity  
367 index due to the combined effects of drought and climate change (i.e., five scenarios of  
368 temperature increase and eCO<sub>2</sub>), still integrated over time to account for recovery:

369

$$370 \quad \text{Severity-climate index} = \text{Severity-drought index}_{\text{drought}} - \text{Severity-drought index}_{\text{drought+CC}} \quad (\text{Eq. 4})$$

371 Because we expect drought to reduce vegetation C stocks, and thus severity-climate  
372 index to be negative, positive values of severity-climate index indicate that changes in climatic  
373 drivers ameliorate the C losses from drought (i.e., buffering effects). Negative values of severity-  
374 climate index indicate that the climate change scenario leads to either greater C losses or losses  
375 that persist for longer amounts of time (i.e., magnitude and/or duration) compared to a simulation  
376 with no climate change (i.e., “control” run).

377

### 378 **3 Results**

379 As a basis for the treatment results presented here, we compared the baseline simulations  
380 (prior to drought or climate change treatments) of the two VDMs against observations, and found  
381 strong model validation at both sites (Table S3, Fig. S1, Supplemental Text A). These models are  
382 well documented and investigated VDMs, with many studies that have looked into parameter  
383 uncertainty (see Supplemental Text A for select references that explore model/parameter  
384 sensitivity).

385 The models displayed varied nonlinear responses to drought, differing substantially in  
386 their behavior and between sites. In general, ED2 shows sensitivity to drought duration  
387 (Hypothesis H1b), while LPJ-GUESS shows a stronger sensitivity to drought intensity  
388 (Hypothesis H1a). ED2’s sensitivity to the duration of drought was mild at Palo Verde (Fig. 2a),  
389 and stronger at EucFACE particularly during the 4-year drought with a strong non-monotonic  
390 pattern (see explanation below) (Fig. 2b). When reporting only percentage of biomass loss, ED2  
391 predicts close to no UCE response at Palo Verde; with a maximum biomass reduction of only  
392 40% during 95% precipitation removal and a 4-year drought event (i.e., UCE). LPJ-GUESS  
393 shows threshold tipping patterns highly sensitive to drought intensity. C loss predicted by LPJ-

394 GUESS at Palo Verde reached a threshold at ~65% drought intensity, after which forests exhibit  
395 strong biomass losses, up to 100% (Fig. 2a). At the EucFACE site, both models predict a critical  
396 threshold of biomass loss at 35%-45% drought intensity, with LPJ-GUESS predicting total  
397 biomass loss (up to 100%) after this drought intensity threshold (Fig. 2b). The EucFACE drought  
398 threshold is lower than that of the seasonally dry mixed tropical forest in Palo Verde.

399 With respect to C loss over a recovering time period (severity-drought index), the two  
400 models predict similar drought responses at Palo Verde (Fig. 2c), but not at EucFACE (Fig. 2d).  
401 At Palo Verde, the similarity between models in severity-drought index reflected longer biomass  
402 recovery time but less biomass loss in the short-term in ED2 relative to LPJ-GUESS, which  
403 predicted greater biomass loss immediately after drought but shorter recovery time. With the  
404 exception of the 1-year drought in ED2, both models predict similar severity-drought index  
405 across a range of UCEs at Palo Verde, via different pathways. The severity-drought index  
406 revealed an exacerbated response to drought duration in ED2 with drought durations greater than  
407 one year (Fig. 2c), compared to when only examining loss in biomass at the time of the event  
408 (Fig. 2a). The “V”-shaped patterns observed particularly in Fig. 2b, arise from interactions  
409 between whole-leaf phenology and stomatal responses to drought in ED2. For drought intensities  
410 lower than 40%, stomatal conductance is reduced but leaves are not fully shed. Leaf respiration  
411 continues, gradually depleting non-structural C pools, followed by a loss of biomass. However,  
412 for higher drought intensities, leaf water potentials quickly become systematically lower than  
413 leaf turgor loss points and tree cohorts shed all their leaves. This strategy represents an  
414 immediate loss of C via leaf shedding, but spares the cohort from slow, respiration-driven  
415 depletion of C stocks.

416

### 417 **3.1 Predicted model responses to UCE droughts combined with increased temperature** 418 **and/or eCO<sub>2</sub>**

419 Relating to our second hypothesis of additional effects of warming and eCO<sub>2</sub>, we tested  
420 15 treatments in total, repeating the five climate change scenarios for each of the three drought  
421 durations. With the addition of climate change impacts, ED2 remained sensitive to the duration  
422 of drought, with warming negatively impacting severity-climate index and most consistently  
423 during 2- and 4-year drought durations. ED2 predicts that during the 2- and 4-year droughts at  
424 EucFACE, losses are exacerbated when accompanied with warming, even with eCO<sub>2</sub>, with 600

425 ppm having a more detrimental impact than the more elevated 800 ppm (Fig. 3b-c). The average  
426 severity-climate index was  $-111.0 \text{ kg C m}^{-2} \text{ yr}$  across all 15 treatments (Table 2). Only during the  
427 1-year drought duration did drought plus warming and  $e\text{CO}_2$  have a buffering effect on C stocks,  
428 seen in four out of our five scenarios but only during relatively modest droughts intensities (Fig.  
429 3a; i.e., positive severity-climate index, see also Table 2).

430 The ED2 simulations of the seasonally dry Palo Verde site (Fig. 3d-f), produced less  
431 frequent negative impacts on drought and climate change driven C losses compared to  
432 EucFACE, with an average severity-climate index of  $-53.9 \text{ kg C m}^{-2} \text{ yr}$  across all 15 treatments  
433 (Table 2). During the 2-year drought, applying +2K with  $e\text{CO}_2$  to 600 ppm showed a slight  
434 buffering effect to droughts and the most consistent positive severity-climate index (Fig. 3e;  
435 Table 2). Interestingly, an increase in only  $e\text{CO}_2$  to 800 ppm (no warming) when applied with the  
436 2- and 4-year droughts resulted in the largest loss in carbon (Fig. 3e-f), larger than the expected  
437 'most severe' scenario; +2K and 800 ppm.

438 Similar to ED2, the LPJ-GUESS model showed a nearly complete negative response in  
439 severity-climate index as a result of UCE drought and scenarios of warming and  $e\text{CO}_2$  at the  
440 EucFACE site (Fig. 3g-i), but mixed and more muted results at Palo Verde (Fig. 3j-l, Table 2).  
441 The average severity-climate index relative to the no climate change control case was  $-95.4$  at  
442 EucFACE and  $-7.8 \text{ kg C m}^{-2} \text{ yr}$  at Palo Verde, both less negative compared to ED2. One notable  
443 pattern was up until a drought intensity threshold of  $\sim 40\%$ , the climate scenarios had no effect or  
444 response in severity-climate index at EucFACE, and the muted response from warming and  
445  $e\text{CO}_2$  Palo Verde, compared to ED2. Surprisingly, the +2K scenario switched the severity-  
446 climate index to positive, compared to the control case (Fig. 3g-i; red lines), potentially a  
447 physiological process in the model to increased temperatures only that signals an anomalous  
448 resiliency response. Similar to the results with no climate change, LPJ-GUESS remained  
449 sensitive to the intensity of drought, with  $\sim 40\%$  precipitation reduction being a threshold.

450 When comparing the VDM responses to increasing drought severity and its interactions  
451 with warming and  $e\text{CO}_2$  (related to conceptual Fig. 1d), ED2 showed a more consistent MO  
452 response during UCEs and with additional warming and  $e\text{CO}_2$  (Fig. 3; negative severity-climate  
453 index), especially at EucFACE, suggesting these ecosystems will remain in a depressed carbon  
454 condition driving vegetation mortality, and/or longer recoveries. LPJ-GUESS produced more  
455 opportunities for SO with climate change. For example, at EucFACE  $\text{CO}_2$  fertilization created

456 small SO periods that then led to MO with increasing drought severities, and at Palo Verde all  
457 +2K and 600 ppm led to a SO (Fig. 3j-l; Table 2).

458 Both models predicted that C losses due to drought interactions with increased  
459 temperature and eCO<sub>2</sub> were less severe at the seasonally dry Palo Verde site compared to the  
460 somewhat less seasonal, more humid EucFACE site (Table 2), which could be attributed to  
461 higher diversity in PFT physiology at Palo Verde. Palo Verde's community composition that  
462 emerged following drought included either three (LPJ-GUESS) or four (ED2) PFTs, while only a  
463 single PFT existed at EucFACE. With rising temperatures under climate change, UCEs will be  
464 hotter and drier. Nine out of the twelve simulations with both +2K and 600 ppm CO<sub>2</sub>, and all but  
465 one +2K and 800 ppm CO<sub>2</sub> produced a negative severity-climate index, implying stronger C  
466 losses and/or longer recovery times when droughts are exacerbated by increasing temperatures  
467 (Table 2).

468

#### 469 **4 Discussion**

470 Vegetation demographic models (VDMs) allowed us to uniquely explore two hypotheses  
471 regarding a range of modeled response of terrestrial ecosystems to unprecedented climate  
472 extremes (UCEs), and setting the stage for the following perspectives to help guide future  
473 research. Key model results indicate strong differences in nonlinearities in C response to extreme  
474 drought *intensities* in LPJ-GUESS and alternatively drought *durations* in ED2 (at one of two  
475 sites), with differences in thresholds between the two models and ecosystems, and only the ED2  
476 model representing impacts from combined intensity and drought (Hypothesis H1c). These  
477 nonlinearities may arise from multiple mechanisms that we begin to investigate here, including  
478 shifts in plant hydraulics or other functional traits, C allocation, phenology, stand size-structure  
479 and/or age demography, and compositional changes, all which vary among ecosystem types. A  
480 critical look of driving model mechanisms, which emerged from the hypothetical drought  
481 simulations used here, are summarized in Table 3. The models also show exacerbated biomass  
482 loss and recovery times in the majority of our scenarios of warming and eCO<sub>2</sub>, supporting  
483 Hypothesis H2. Below, we discuss the underlying mechanisms that drive simulated ecosystem  
484 response to UCEs using the models and sites as conceptual "experimental tools" and  
485 observational evidence from the literature. We focus on two temporal stages of the UCE: The  
486 pre-drought ecosystem stage characterized as the quasi-stable state of the ecosystem prior to a



487 UCE, which can mediate ecosystem resistance and disturbance impact, and the post-drought  
488 recovery stage (Table 1).

489

#### 490 **4.1 The role of ecosystem processes and states prior to UCEs**

##### 491 **4.1.1 The role of phenology and phenological strategies prior to UCEs:**

492 Observations show that diversity of deciduousness contributes to successful alternative  
493 strategies for tropical forest response to water stress (Williams et al., 2008). For example, during  
494 the severe 1997 El Nino drought, brevi-deciduous trees and deciduous stem-succulents within a  
495 tropical dry site in Guanacaste Costa Rica retained leaves during the extreme wet-season  
496 drought, behaving differently than during normal dry seasons (Borchert et al., 2002). Both  
497 models here predict that neither seasonal deciduousness, nor drought-deciduous phenology at the  
498 seasonally dry tropical forest, Palo Verde (which consists of trees with different leaf  
499 phenological strategies), act to buffer the forest from a large drop in LAI during UCEs (Fig. S1a-  
500 b). Even with this large decrease in LAI, ED2 predicted a very weak biomass loss at the time of  
501 UCEs (Fig. 2a), suggesting large-scale leaf loss is not a direct mechanism of plant mortality in  
502 ED2. Leaf loss is one component of total carbon turnover flux equations in terrestrial models, in  
503 addition to woody loss, fine-roots, and reproductive tissues. Having a better understanding of  
504 when extreme levels of phenological turnover contribute to stand-level mortality could be  
505 improved. Among other turnover hypothesis explored, Pugh et al. (2020) found that phenological  
506 turnover fluxes were just as important as mortality fluxes in driving forest turnover time in the  
507 VDMs: LPJ-GUESS, CABLE-POP, ORCHIDEE, but not the LSM JULES. At the EucFACE  
508 site prior to the simulated extreme drought, LPJ-GUESS displayed strong inter-annual variability  
509 in LAI (Fig. S1a-b). This capability of large swings in LAI (5.8 to 0.8) by LPJ-GUESS could  
510 contribute to model uncertainty and the considerable mortality response at EucFACE. Modeled  
511 LAI was the largest source of variability in another ecosystem model, CABLE, when evaluating  
512 the simulated response to CO<sub>2</sub> fertilization (Li et al., 2018). VDMs could be improved by better  
513 capturing different plant phenological responses to UCEs by better representing a range of leaf-  
514 level morphological and physiological characteristics relevant to plant-water relations such as  
515 leaf age, retention of young leaves even during extreme droughts, (Borchert et al., (2002)), and  
516 variation in hydraulic traits as a function of leaf habit (Vargas et al., (2021)) (Table 3). Two such

517 examples are seen in the FATES model where the possibility for “trimming” the lowest leaf  
518 layer can occur when leaves are in negative carbon balance due to light limitation thus  
519 optimizing maintenance costs and carbon gain, as well as leaf age classifications providing  
520 variations in leaf productivity and turnover.

521

#### 522 **4.1.2 The role of plant hydraulics prior to UCEs:**

523 Susceptibility of plants to hydraulic stress is one of the strongest determinants of  
524 vulnerability to drought, with loss of hydraulic conductivity being a major predictor of drought  
525 mortality in temperate (McDowell et al., 2013; Anderegg et al., 2015; Sperry and Love, 2015;  
526 Venturas et al., 2021) and tropical forests (Rowland et al., 2015; Adams et al., 2017b), as well as  
527 a tractable mortality mechanism to represent in process-based models (Choat et al., 2018,  
528 Kennedy et al., 2019). Both LPJ-GUESS and ED2 exhibited a wide range in amount and pattern  
529 of plant-available-water prior to drought (Fig. S1c-d), contributing to large differences in UCE  
530 response. LPJ-GUESS, which does not simulate hydrodynamics, predicted lower total plant-  
531 available-water at both sites compared to ED2, and subsequently simulated greater mortality and  
532 a greater increase in plant-available-water right after the UCEs as a result of less water demand.  
533 Due to ED2 using a static mortality threshold from conductivity loss (88%), it likely does not  
534 accurately reproduce the wide range of observations of drought-induced mortality. In ED2, large  
535 trees, with longer distances to transport water, were at higher risk and suffered higher mortality  
536 (Fig. 4), demonstrating how stand demography, size structure, and tapering of xylem conduits  
537 can play an important role in ecosystem models (Petit et al., 2008; Fisher et al., 2018). Of the  
538 VDMs that are beginning to incorporate a continuum of hydrodynamics (e.g., ED2 (described in  
539 Methods 2.1 section) and FATES-HYDRO (Fang et al., 2022, based on Christoffersen et al.,  
540 2016), they are able to solve for transient water from soils to roots, through the plant and connect  
541 with transpiration demands. Therefore, instead of the plant water stress function being based on  
542 soil water potentials, it is replaced with more realistic connections with leaf water potentials.  
543 Mortality is then caused by hydraulic failure via embolism controlled by the critical water  
544 potential ( $P_{50}$ ) that leads to 50% loss of hydraulic conductivity. For advancements in tree level  
545 hydrodynamic modeling see the FETCH3 model (Silva et al., 2022), for justification for plant  
546 hydrodynamics in conjunction with multi-layer vertical canopy profiles see Bonan et al., (2021).  
547 There are strong interdependencies and related mechanisms connecting both hydraulic failure

548 (e.g., low soil moisture availability) and C limitation (e.g., stomatal closure) during drought  
549 (McDowell et al., 2008; Adams et al., 2017b), and these interactions should be incorporated in  
550 ecosystem modeling and further explored (Table 3).

#### 551 **4.1.3. The role of carbon allocation prior to UCEs:**

552 Plants have a variety of strategies to buffer vulnerability to water and nutrient stress  
553 caused by extreme droughts, such as allocating more C to deep roots (Joslin et al., 2000; Schenk  
554 and Jackson, 2005), investing in mycorrhizal fungi (Rapparini and Peñuelas, 2014), or reducing  
555 leaf area without shifting leaf nutrient content (Pilon et al., 1996). Alternatively, presence of  
556 deep roots doesn't necessarily lead to deep soil moisture utilization, as seen in a 6-year  
557 Amazonian throughfall exclusion experiment where deep root water uptake was still limited,  
558 even with high volumetric water content (Markewitz et al., 2010). Elevated CO<sub>2</sub> alone will  
559 enhance growth and water-use efficiency (Keenan et al., 2013), reducing susceptibility to  
560 drought. However, such increased productivity within a forest stand, and associated structural  
561 overshoot during favorable climate windows, can also be reversed by increased competition for  
562 light, nutrients, and water during unfavorable UCEs – potentially leading to mortality overshoot  
563 (Fig. 1d) and higher C loss. Mortality overshoot, as a result of structural overshoot, could be an  
564 explanation for the negative severity-climate index (i.e., C loss) in the majority of eCO<sub>2</sub>-only  
565 simulations (18 out of 24 scenarios; Table 2).

566 Effects of CO<sub>2</sub> fertilization on plant C allocation strategies are uncertain. As a result,  
567 ecosystem models differ in their assumptions on controls of C allocation in response to eCO<sub>2</sub>,  
568 leading to divergent plant C use efficiencies (Fleischer et al., 2019). Global scale terrestrial  
569 models are beginning to include optimal dynamic C allocation schemes, over fixed ratios, that  
570 account for concurrent environmental constraints on plants, such as water, and adjust allocation  
571 based on resource availability such as in LM3-PPA (Weng et al., 2015), but the representation of  
572 C allocation is still debated and progressing (De Kauwe et al., 2014; Montané et al., 2017; Reyes  
573 et al., 2017). Options for carbon allocation strategies can be based on the allometric partitioning  
574 theory (i.e., allocation follows a power allometry function between plant size and organs which  
575 is insensitive to environmental conditions; Niklas, 1993), as an alternative to ratio-based optimal  
576 partitioning theory (i.e., allocation to plant organs based on the most limiting resources)  
577 (McCarthy and Enquist, 2007) or fixed ratios (Table 3), and the strategies should be further  
578 investigated particularly due to VDMs substantial use of allometric relationships. A meta-

579 analysis of 164 studies found that allometric partitioning theory outperformed optimal  
580 partitioning theory in explaining drought-induced changes in C allocation (Eziz et al., 2017).  
581 Further eco-evolutionarily-based approaches such as optimal response or game-theoretic  
582 optimization, as well as entropy-based approaches are useful when wanting to simulate higher  
583 levels of complexity (reviewed in Franklin et al. 2012). With more frequent UCEs and the need  
584 for plants to reduce water consumption, a shift in the optimal strategy of allocation between  
585 leaves and fine roots should change. The goal functions (e.g., fitness proxy) used in optimal  
586 response modeling can account for these shifts in costs and benefits of allocation between all  
587 organs (Franklin et al. 2009, 2012).

588

#### 589 **4.1.4 The role of plant carbon storage prior to UCEs:**

590 Studies of neotropical and temperate seedlings show that pre-drought storage of non-  
591 structural carbohydrates (NSCs) provides the resources needed for growth, respiration  
592 osmoregulation, and phloem transport when stomata close during subsequent periods of water  
593 stress (Myers and Kitajima, 2007; Dietze and Matthes, 2014; O'Brien et al., 2014). Furthermore,  
594 direct correlations have been shown between NSC depletion and embolism accumulation, and  
595 the degree of pre-stress reserves and utilization of soluble sugars (Tomasella et al., 2020). The  
596 amount of NSC storage required to mitigate plant mortality during C starvation and interactions  
597 with hydraulic failure from severe drought is difficult to quantify, due to the many roles of NSCs  
598 in plant function and metabolism (Dietze and Matthes, 2014). For example, NSCs were not  
599 depleted after 13 years of experimental drought in the Brazilian Amazon (Rowland et al., 2015).  
600 As atmospheric CO<sub>2</sub> increases with climate change, NSC concentrations may increase, as seen in  
601 manipulation experiments (Coley, 2002), but interactions with heat, water stress, enhanced leaf  
602 shedding, and nutrient limitation complicates this relationship, and needs to be further explored.  
603 Despite the recognition of the critical role that plant hydraulic functioning and NSCs play in tree  
604 resilience to extremes, knowledge gaps and uncertainties preclude fully incorporating these  
605 processes into ecosystem models.

606 Compared to ED2, LPJ-GUESS predicted low plant carbon storage (a model proxy for  
607 NSCs) prior to and during drought, and at times became negative, thereby creating C costs (Fig.  
608 S2a-b), leading to C starvation and potentially explaining the larger biomass loss in LPJ-GUESS  
609 at both sites. Alternatively, ED2 maintained higher levels of NSCs providing a buffer to stress,

610 and mitigating the negative effects of drought. Maintenance of NSCs in ED2, even during  
611 prolonged drought (at EucFACE) is due to: (1) trees resorbing a fraction of leaf C during leaf  
612 shedding, (2) no maintenance costs for NSC storage in the current version, and (3) no allocation  
613 of NSCs to structural growth until NSC storage surpasses a threshold (the amount of C needed to  
614 build a full canopy of leaves and associated fine roots), allowing for a buffer to accumulate. In  
615 LPJ-GUESS, accumulation and depletion of NSC is recorded as a ‘C debt’ being paid back in  
616 later years. The contrasting responses of the two models to drought, and the likely role of NSCs  
617 in explaining differences in model behavior, highlights the need to better understand NSC  
618 dynamics and to accurately represent the relevant processes in models (Richardson et al., 2013;  
619 Dietze and Matthes, 2014). More observations of C accumulation patterns and how/where NSCs  
620 drive growth, respiration, transport and cellular water relations would enable a more realistic  
621 implementation of NSC dynamics in models (Table 3).

622

#### 623 **4.1.5 Role of functional trait diversity prior to UCEs:**

624 Currently LPJ-GUESS simulates the Palo Verde community using three PFTs, while ED2 uses  
625 four PFTs that differ in photosynthetic and hydraulic traits. The community composition simulated by  
626 ED2 is shown to be more resistant to UCEs compared to LPJ-GUESS (Fig. 5), perhaps due to  
627 relatively higher functional diversity (via more PFTs with additional phenological and hydraulic  
628 diversity). This additional diversity helps to buffer ecosystem response to drought by allowing more  
629 tolerant PFTs to benefit from reductions in less-tolerant PFTs, thus buffering reductions in ecosystem  
630 function (Anderegg et al., 2018). Higher diversity ecosystems were found to protect individual species  
631 from negative effects of drought (Aguirre et al., 2021) and enhance productivity resilience following  
632 wildfire (Spasojevic et al., 2016); thus, functionally diverse communities may be key to enhancing  
633 tolerance to rising environmental stress.

634 Recent efforts to consolidate information on plant traits (Reich et al., 2007; Kattge et al., 2011)  
635 have contributed to identifying relationships that can impact community-level drought responses  
636 (Skelton et al., 2015; Anderegg et al., 2016a; Uriarte et al., 2016; Greenwood et al., 2017), such as  
637 life-history characteristics, and strategies of resource acquisition and conservation as predictors of  
638 ecosystem resistance (MacGillivray et al., 1995; Ruppert et al., 2015). While adding plant trait  
639 complexity in ESMs may be required to accurately simulate key vegetation dynamics, it necessitates  
640 more detailed parameterizations of processes that are not explicitly resolved (Luo et al., 2012). Further

641 investigation of how VDMs represent interactions leading to functional diversity shifts is crucial to  
642 this issue. Enquist and Enquist, (2011), as an example, show that long-term patterns of drought (20-  
643 years) have led to increases in drought-tolerant dry forest species, which could modulate resistance to  
644 future droughts. Higher diversity of plant physiological traits and drought-resistance strategies is  
645 expected to enhance community resistance to drought, and models should account for shifts in diverse  
646 functionality (Table 3).

647

## 648 **4.2 The role of ecosystem processes and states in post-UCE recovery**

### 649 **4.2.1 The role of soil water resources post-UCes:**

650 Our simulation results generally demonstrated a fast recovery of plant-available-water  
651 and LAI at both sites (Fig. S1). Annual plant-available-water substantially increased right after  
652 drought by an average of 163 mm at Palo Verde and 213 mm at EucFACE in the LPJ-GUESS  
653 simulations, compared to much lower increases in ED2 (50 mm and 12 mm at Palo Verde and  
654 EucFACE). This increase in available water post-drought can be attributed to reduced stand  
655 density and water competition (Fig. S2c-d; diamonds vs. circles), alleviating the demand for soil  
656 resources (water) and subsequent stress, which has also been shown in observations (McDowell  
657 et al., 2006; D'Amato et al., 2013). After large canopy tree mortality events there can be  
658 relatively rapid recovery of forest biogeochemical and hydrological fluxes (Biederman et al.,  
659 2015; Anderegg et al., 2016b; Biederman et al., 2016). These crucial fluxes strongly influence  
660 plant regeneration and regrowth, which can buffer ecosystem vulnerability to future extreme  
661 droughts. However, this enhanced productivity has a limit. In a scenario where UCEs continue to  
662 intensify, causing greater reductions in soil water and reduced ecosystem recovery potential, the  
663 SO growth that typically occurs after UCEs may be dampened (Fig. 1d). In water-limited  
664 locations, similar to the dry forest sites used here, initial forest recovery from droughts were  
665 faster due to thinning induced competitive-release of the surviving trees, and shallow roots not  
666 having to compete with neighboring trees for water, allowing for more effective water user  
667 (Tague and Moritz, 2019), stressing the importance of root competition and distribution in  
668 models (Goulden and Bales, 2019). Tague and Moritz, (2019) also reported that this increased  
669 water use efficiency and SO ultimately lead to water stress and related declines in productivity,  
670 similar to the MO concept (Jump et al., 2017; McDowell et al., 2006). Since a core strength of

671 VDMs is predicting stand demography during recovery, improved quantification of density-  
672 dependent competition following stand dieback would be beneficial for model benchmarking  
673 (Table 3).

674

#### 675 **4.2.2 The role of lagged turnover and secondary stressors post-UCEs:**

676 Time lags in forest compositional response and survival to drought could indicate  
677 community resistance or shifts to more competitive species and competitive exclusion. During a  
678 15-year recovery period from extreme drought at Palo Verde, LPJ-GUESS predicted an increase  
679 in stem density (stems  $\text{m}^2 \text{yr}^{-1}$ ) (Fig. S2c) compared to ED2, which predicted almost no impact in  
680 stem recovery. The mortality “spike” in ED2 due to drought was muted and slightly delayed,  
681 contributing to ED2’s lower biomass loss and more stable behavior of plant processes over time  
682 at Palo Verde. At EucFACE, both models exhibited a pronounced lag effect in stem turnover  
683 response, i.e. ~8-12 years after drought (Fig. S2d). After about a decade, strong recoveries and  
684 increased stem density occurred, which in ED2 was followed by delayed mortality/thinning of  
685 stems. Delayed tree mortality after droughts is common due to optimizing carbon allocation and  
686 growth (Trugman et al., 2018), but typically only up to several years post-drought, not a decade  
687 or more as seen in the model.

688 The versions of the VDMs used here do not directly consider post-drought secondary  
689 stressors such as infestation by insects or pathogens, and the subsequent repair costs due to stress  
690 damage, which could substantially slow the recovery of surviving trees. Forest ecologists have  
691 long recognized the susceptibility of trees under stress, particularly drought, to insect attacks and  
692 pathogens (Anderegg et al., 2015). Tight connections between drought conditions and increased  
693 mountain pine beetle activity have been observed (Chapman et al., 2012; Creeden et al., 2014),  
694 and can ultimately lead to increased tree mortality (Hubbard et al., 2013). Leaf defoliation is a  
695 major concern from insect outbreaks following droughts, and can have large impacts on C  
696 cycling, plant productivity, and C sequestration (Amiro et al., 2010; Clark et al., 2010; Medvigy  
697 et al., 2012). Implementing these secondary stressors in models could slow the rate of post-UC  
698 recovery and lead to increased post-UCEs tree mortality.

699

### 700 4.2.3 The role of stand demography post-UCEs:

701 Change in stand structure is an important model process to capture, because large trees  
702 have important effects on C storage, community resource competition, and hydrology  
703 (Wullschleger et al., 2001) (Table 3), and maintaining a positive carbohydrate balance is  
704 beneficial in sustaining (or repairing) hydraulic viability (McDowell et al., 2011). There is  
705 increasing evidence, both theoretical (McDowell and Allen, 2015) and empirical (Bennett et al.,  
706 2015; Rowland et al., 2015; Stovall et al., 2019), that large trees (particularly tall trees with high  
707 leaf area) contribute to the dominant fraction of dead biomass after drought events. Under rising  
708 temperatures (and decreasing precipitation), VPD will increase, leading to a higher likelihood of  
709 large tree death (Eamus et al., 2013; Stovall et al., 2019), driving MO events as hypothesized in  
710 Fig. 1d. Consistent with this expectation, ED2 predicted that the largest trees (>100 cm)  
711 experienced the largest decreases in basal area to compared to all other size classes (Fig. 4). This  
712 drought-induced partial dieback and mortality of large dominant trees has substantial impacts on  
713 community-level C dynamics, as long-term sequestered C is liberated during the decay of new  
714 dead wood (Palace et al., 2008; Potter et al., 2011). In ED2, the intermediate size class (60 - 80  
715 cm) increased in basal area following large-tree death, taking advantage of the newly open  
716 canopy space. However, small size classes do not necessarily benefit from canopy dieback. For  
717 example, in a dry tropical forest, prolonged drought led to a decrease in understory species and  
718 small-sized stems (Enquist and Enquist, 2011).

719 Due to VDMs being able to exhibit dynamic biogeography they are more useful at  
720 predicting shifts in community composition beyond LSMs capabilities. Further areas of  
721 advancement (described in Franklin et al. (2020)) is including models of natural selection, self-  
722 organization, and entropy maximization which can substantially improve community dynamic  
723 responses in varying environments such as UCEs. Eco-evolutionary optimality (EEO) theory can  
724 also help improve functional trait representation in global process-based models (reviewed in  
725 Harrison et al., 2021), through hypotheses in plant trait trade-offs and mechanistic links between  
726 processes such as resource demand, acquisition, and plant's competitiveness and survival; traits  
727 associated with high degrees of sensitivity in models. The power of prognostic VDMs to predict  
728 shifts in demography and community migration with climate change is large, but rarely is being  
729 constrained with plant-level EEO theory, and thus will likely need to use stand level competition  
730 and coexistence principles of how plants self-organize (Franklin et al. 2020).



731

#### 732 **4.2.4 The role of functional trait diversity & plant hydraulics post-UCEs:**

733 In field experiments, higher disturbance rates have shifted the recovery trajectory and  
734 competition of the plant community towards one that is composed of opportunistic, fast-growing  
735 pioneer tree species, grasses (Shiels et al., 2010; Carreño-Rocabado et al., 2012), and/or  
736 deciduous species, as also seen in model results (Hickler et al., 2004). In the treatments presented  
737 here, deciduous PFT types were also the strongest to recover after 15 years in both models,  
738 surpassing pre-drought values (Fig. 5). It should be noted that ED2 exhibited a strong recovery in  
739 the evergreen PFT as well, inconsistent with the above literature (Fig. 5b). PFTs in ED2 respond  
740 to drought conditions via stomatal closure and leaf shedding, buffering stem water potentials  
741 from falling below a set mortality threshold (i.e., 88% of loss in conductivity). This conductivity  
742 threshold may need to be reconsidered if further examination reveals an unrealistic advantage  
743 under drought conditions for evergreen trees, which exhibited a lower impact from droughts  
744 (compared to deciduous and brevi-deciduous PFTs) in ED2. Nitrogen cycling feedbacks were  
745 not investigated here, but could also be an explanation for a strong evergreen PFT recovery.

746 Recovery of surviving trees could be hindered by the high cost of replacing damaged  
747 xylem associated with cavitation (McDowell et al., 2008; Brodribb et al., 2010). Many studies  
748 have identified “drought legacy” effects of delayed growth or gross primary productivity  
749 following drought (Anderegg et al., 2015; Schwalm et al., 2017) and the magnitude of these  
750 legacies across species correlates with the hydraulic risks taken during drought itself (Anderegg  
751 et al., 2015). The conditions under which xylem can be refilled remain controversial, but it seems  
752 likely that many species, particularly gymnosperms, may need to entirely replace damaged  
753 xylem (Sperry et al., 2002), and trees worldwide operate within narrow hydraulic safety margins,  
754 suggesting that trees in all biomes are vulnerable to drought (Choat et al., 2012). The amount of  
755 damaged xylem from a given drought event and recovery rates also vary across trees of different  
756 sizes (Anderegg et al., 2018).

757 Plasticity in nutrient acquisition traits, intraspecific variation in plant hydraulic traits  
758 (Anderegg et al., 2015), and changes in allometry (e.g., Huber values) can have large effects on  
759 acclimation to extreme droughts. This suggests some capacity for physiological adaptation to  
760 extreme drought, as seen by short-term negative effects from drought and heat extremes being

761 compensated for in the longer term (Dreesen et al., 2014). Still, given the shift towards more  
762 extreme droughts with climate change, vegetation mortality thresholds are likely to be exceeded,  
763 as reported in Amazonian long-term plots where mortality of wet-affiliated genera has increased  
764 while simultaneously new recruits of dry-affiliated genera are also increasing (Esquivel-Muelbert  
765 et al., 2019). Increasing occurrences of heat events, water stress and high VPD will lead to  
766 extended closure of stomata to avoid cavitation, progressively reducing CO<sub>2</sub> enrichment benefits  
767 (Allen et al., 2015). Where CO<sub>2</sub> fertilization has been seen to partially offset the risk of  
768 increasing temperatures, the risk response was mediated by plant hydraulic traits (Liu et al.,  
769 2017) using a soil–plant–atmosphere continuum (SPAC) model, yet interactions with novel  
770 extreme droughts were not considered. The VDM simulations suggest that the combination of  
771 elevated warming and potential structural overshoot from eCO<sub>2</sub> (or inaccurate representation in  
772 NSCs allocation/usage priority) will exacerbate consequences of UCEs by reductions in both C  
773 stocks and post-drought biomass recovery speeds (Fig. 3). Therefore, future UCE recovery may  
774 not be easily predicted from observations of historical post-disturbance recovery. An associated  
775 area for further investigation is to better understand the hypothesized interplay between  
776 amplified mortality from hotter UCEs followed by structural overshoot regrowth during wetter  
777 periods (Fig. 1d), which could potentially lead to continual large swings in MO and SO and  
778 vulnerable net ecosystem C fluxes through time (Table 3).

779

## 780 **5 Summary of perspectives for model advancement**

781 Model limitations and unknowns exposed by our simulations and literature review  
782 highlight current challenges in our ability to understand and forecast UCE effects on ecosystems.  
783 These limitations reflect a general lack of empirical experiments focused on UCEs. Insufficient  
784 data means that relevant processes may currently be poorly represented in models, and models  
785 may then misrepresent C losses during UCEs. The two VDMs used here had different  
786 sensitivities to drought duration or intensity, and CO<sub>2</sub> and warming interactions, indicating the  
787 wide variety of unknowns and plausible options when trying to represent future UCEs that still  
788 needs to be narrowed down (Fig. 1d). These model uncertainties could potentially be addressed  
789 by improved datasets on thresholds of conductivity loss at high drought intensities, the role of  
790 trait diversity (e.g., different strategies of drought deciduousness and EEO theory) in buffering  
791 ecosystem drought responses, and a better grasp of allocation to plant C storage stocks before,

792 during, and after multi-year droughts. Our study takes some initial steps to identify and assess  
793 model gaps in terms of mechanisms and magnitudes of responses to UCEs, which can then be  
794 used to inform and develop field experiments targeting key knowledge gaps as well as to  
795 prioritize ongoing model development (Table 3). Our intention was not to do an exhaustive list  
796 of UCE simulation experiments, and additional modeling perturbations and experiments would  
797 be useful outcomes of future studies. For example, we begin to investigate duration of droughts  
798 but we did not consider frequency of back-to-back UCEs. Using VDMs as hypothesis testing  
799 tools offers strong potential to drive progress in improving our understanding of terrestrial  
800 ecosystem responses to UCEs and climate feedbacks, while informing the development of the  
801 next generation of models.

802 *Code Availability.* The source code for the ED2 model can be downloaded and available publicly  
803 at <https://github.com/EDmodel/ED2>. The source code for the LPJ-GUESS model can be  
804 downloaded and available publicly at <http://web.nateko.lu.se/lpj-guess/download.html>. All model  
805 simulation data will be available in a Dryad repository.  
806

807 *Data Availability.* Authors received the required permissions to use the site level meteorological  
808 data used in this study. Otherwise, no ecological or biological data were used in this study.  
809

810 *Author Contributions.* JH wrote the manuscript with significant contributions from AR, BS, JD,  
811 DM, with input and contributions from all authors. XX and MM were the primary leads running  
812 the model simulations, with model assistance and strong feedback from DM and BS. All authors  
813 made contributions to this article, and agree to submission.  
814

815 *Competing Interests.* The contact author has declared that neither they nor their co-authors have  
816 any competing interests.  
817

818 *Special Issue Statement.* Special Issue titled “Ecosystem experiments as a window to future  
819 carbon, water, and nutrient cycling in terrestrial ecosystems”  
820

821 *Financial Support:* Funding for the meetings that facilitated this work was provided by NSF-  
822 DEB-0955771: An Integrated Network for Terrestrial Ecosystem Research on Feedbacks to the  
823 Atmosphere and ClimatE (INTERFACE): Linking experimentalists, ecosystem modelers, and  
824 Earth System modelers, hosted by Purdue University; as well as Climate Change Manipulation  
825 Experiments in Terrestrial Ecosystems: Networking and Outreach (COST action ClimMani –  
826 ES1308), led by the University of Copenhagen. J.A. Holm’s time was supported as part of the  
827 Next Generation Ecosystem Experiments-Tropics, funded by the U.S. Department of Energy,  
828 Office of Science, Office of Biological and Environmental Research under Contract DE-AC02-  
829 05CH11231. AR acknowledges funding from CLIMAX Project funded by Belmont Forum and  
830 the German Federal Ministry of Education and Research (BMBF). BS and MM acknowledge  
831 support from the Strategic Research Area MERGE. W.R.L.A. acknowledges funding from the  
832 University of Utah Global Change and Sustainability Center, NSF Grant 1714972, and the  
833 USDA National Institute of Food and Agriculture, Agricultural and Food Research Initiative  
834 Competitive Programme, Ecosystem Services and Agro-ecosystem Management, grant no. 2018-  
835 67019-27850. JL acknowledges support from the Northern Research Station of the USDA Forest  
836 Service (agreement 16-JV-11242306-050) and a sabbatical fellowship from sDiv, the Synthesis  
837 Centre of iDiv (DFG FZT 118, 202548816). CDA acknowledges support from the USGS Land  
838 Change Science R&D Program.  
839

840 *Acknowledgements.* We thank Belinda Medlyn and David Ellsworth of the Hawkesbury Institute  
841 for the Environment, Western Sydney University, for providing the meteorological forcing data  
842 series for the EucFACE site, a facility supported by the Australian Government through the  
843 Education Investment Fund and the Department of Industry and Science, in partnership with  
844 Western Sydney University.  
845

846 **Table 1.** Hypothesized plant processes and ecosystem state variables affecting pre-drought  
847 resistance and post-drought recovery in the context of unprecedented climate extremes (UCEs).  
848 The “Included in Model?” column indicates which processes or state variables are represented in  
849 each of the two models studied in this paper. The mechanisms listed in the two right columns  
850 refer to real-world ecosystems and are not necessarily represented in the ED2 and LPJ-GUESS  
851 models. Contents of the table are based on a non-exhaustive literature review, expert knowledge,  
852 and modeling results presented here. Symbols refer to the following literature sources: \*  
853 Borchert et al., 2002; Williams et al., (2008); \*\* Dietze and Matthes, (2014); O’Brien et al.,  
854 2014; \*\*\* ENQUIST and ENQUIST, (2011); Greenwood et al., (2017); Powell et al., (2018); ^  
855 Rowland et al., (2015); McDowell et al., (2013); Anderegg et al., (2015); ^^ Joslin et al., 2000;  
856 Markewitz et al., (2010); ^^^ Powell et al., (2018); ^^^^ Bennett et al., (2015); Rowland et al.,  
857 (2015); ~ Hubbard et al., (2013); ~ ~ McDowell et al., (2006); D’Amato et al., (2013); + Zhu et  
858 al., (2018); Vargas et al., (2021); % Trugman et al., (2019); %% Franklin et al., (2012); %%  
859 Franklin et al., (2020).

Process or State Variable	Included in model?	Mechanisms affecting pre-UCE drought resistance influencing impact	Mechanisms affecting post-UCE drought recovery
Processes			
1) Phenology Schemes	ED2: Yes LPJ-G: Yes	- Leaf area and metabolic activity modulates vulnerability to death - Drought-deciduousness reduces vulnerability to drought *, with higher water potential at turgor loss point and less leaf vulnerability to embolism +	- Leaf lifespan tends to increase from pioneer to late-successional species in some ecosystems (e.g., tropical forests) and is a balance between C gain and its cost
2) Plant Hydraulics	ED2: Yes LPJ-G: No	- Cavitation resistance traits ^ - Turgor loss, hydraulic failure (stem embolism) lead to increased plant mortality and enhanced vulnerability to secondary stressors.	- Replacement cost of damaged xylem slows recovery of surviving trees
3) Dynamic Carbon Allocation	ED2: Yes LPJ-G: Yes	- Increased root allocation could offset soil water deficit under gradual onset of drought ^^ - Leaf C allocation strategies should be connected to hydraulic processes %	- Allocation among fine roots, xylem, & leaves affects recovery time & GPP/LAI trajectory - Eco-evolutionary optimality theory %%

4) Non-Structural Carbohydrate (NSC) Storage	ED2: Yes LPJ-G: Yes	- NSCs buffer C starvation mortality due to reduced primary productivity. - Maintenance of hydraulic function & avoiding hydraulic failure **	- Low NSC could increase vulnerability to secondary stressors during recovery
State Variables			
1) Plant-Soil Water Availability	ED2: Yes LPJ-G: Partly	- Low soil water potential increases risk of tree C starvation, turgor loss and hydraulic failure	- After stand dieback reduced demand for soil resources &/or reduced shading - Increased soil water enhances regeneration/ regrowth, buffers vulnerability to long-term drought ~ ~
2) Plant Functional Diversity	ED2: Yes LPJ-G: Yes	- Presence of drought-tolerant species modulates resistance at community level. - Shallow-rooting species more vulnerable ^^ ^***	- Changed resource spectra shift competitive balance in favor of grasses and pioneer trees
3) Stand Demography	ED2: Yes LPJ-G: Yes	- Larger tree size enhances vulnerability to drought and secondary stressors due to higher maintenance costs ^^ ^^	- Mortality of canopy individuals favors understory species and smaller size-classes - Self-organizing principles %%%
4) Compounding Stressors	ED2: No LPJ-G: No	- Reduced resistance to insects and pathogens due to physiological/mechanical/ hydraulic damage & depletion of NSC	- Infestation by insects and pathogens, repair of damage due to secondary stressors, slows recovery of surviving trees ~

861 **Table 2** Impact of eCO<sub>2</sub> and/or temperature on the severity-climate index (kg C m<sup>-2</sup> yr) relative  
862 to drought treatments with no additional warming or eCO<sub>2</sub>, for both models, and both sites seen  
863 in Fig. 3. Quantified as average and minimum severity-climate index across all 20 drought  
864 intensities for step-change scenarios of warming and eCO<sub>2</sub>. The percentage of each scenario that  
865 was negative in severity-climate index (i.e., decreases in C loss). Green values represent positive  
866 severity-climate index.

<i>EucFACE</i>		<i>ED2</i>			<i>LPJ-GUESS</i>		
		Average severity-climate index	Largest severity-climate index	% climate scenario was negative	Average severity-climate index	Largest severity-climate index	% climate scenario was negative
1 year	600 ppm	2.2	0.0	33.3	-74.6	-396.6	36.8
	800 ppm	-10.6	-73.0	50.0	-124.1	-416.0	57.9
	2K	2.3	-0.5	16.7	21.3	-20.8	15.8
	2K, 600 ppm	0.5	-8.2	61.1	-67.5	-201.5	78.9
	2K, 800 ppm	1.8	-0.4	22.2	-145.9	-400.1	47.4
2 year	600 ppm	-105.6	-456.7	77.8	-85.2	-260.6	63.2
	800 ppm	-199.0	-522.9	83.3	-106.3	-350.1	42.1
	2K	-10.3	-34.7	77.8	14.2	-35.2	31.6
	2K, 600 ppm	-204.9	-666.1	77.8	-47.6	-128.8	84.2
	2K, 800 ppm	-12.4	-61.6	50.0	-167.0	-421.9	68.4
4 year	600 ppm	-125.5	-306.2	83.3	-122.6	-277.4	94.7
	800 ppm	-277.1	-423.3	100.0	-212.2	-523.7	89.5
	2K	-61.8	-188.6	72.2	12.9	-13.8	31.6
	2K, 600 ppm	-385.9	-674.2	94.4	-79.1	-197.3	94.7
	2K, 800 ppm	-277.9	-737.7	72.2	-247.0	-503.8	100.0
Average		-111.0	-277.0	64.8	-95.4	-276.5	62.5
<i>Palo Verde</i>		<i>ED2</i>			<i>LPJ-GUESS</i>		
1 year	600 ppm	-1.6	-6.2	77.8	-11.0	-32.4	78.9
	800 ppm	6.7	-0.2	11.1	-39.2	-154.0	100.0
	2K	-1.0	-15.3	38.9	-33.4	-75.1	100.0
	2K, 600 ppm	2.5	-1.1	22.2	6.5	-4.6	52.6
	2K, 800 ppm	-6.6	-16.6	77.8	-121.1	-237.7	100.0
2 year	600 ppm	15.1	-16.7	38.9	27.3	-6.0	10.5
	800 ppm	-229.2	-756.6	66.7	20.6	-17.2	26.3
	2K	-8.2	-71.8	50.0	32.0	-12.7	15.8
	2K, 600 ppm	24.8	-5.7	11.1	36.2	-1.2	5.3
	2K, 800 ppm	-152.9	-348.1	77.8	8.0	-54.5	36.8
4 year	600 ppm	-11.1	-37.3	94.4	3.4	-25.1	26.3
	800 ppm	-260.2	-694.8	94.4	-25.2	-132.6	57.9
	2K	-39.0	-133.8	66.7	-7.7	-45.9	68.4
	2K, 600 ppm	1.0	-16.4	38.9	6.1	-4.1	31.6
	2K, 800 ppm	-148.5	-429.3	83.3	-20.0	-75.5	78.9
Average		-53.9	-170.0	56.7	-7.8	-58.6	52.6

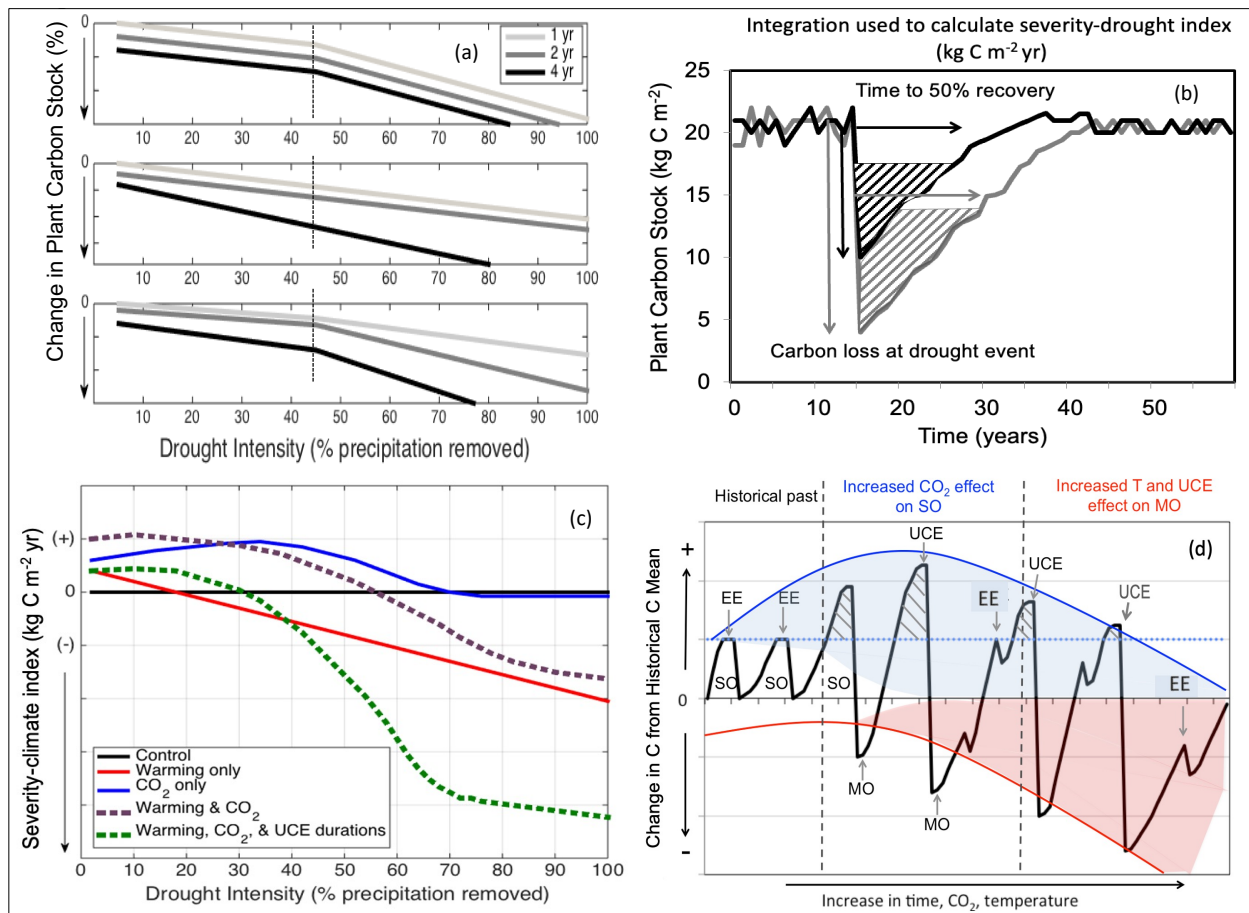
867

868 **Table 3** Summary of suggested critical look of driving mechanisms (e.g., ecosystem or plant  
 869 processes and state variables) which emerged from the hypothetical drought simulations used  
 870 here to explore for future research in manipulation experiments, data collection, and model  
 871 development and testing, as related to furthering our understanding of UCE resistance and  
 872 recovery.

<b>UCE Drought Resistance &amp; Recovery Summary</b>	
<b>Processes</b>	<b>Suggestions of driving mechanisms to further explore in data and models</b>
1) Phenology Schemes	Represent morphological and physiological traits relevant to plant-water relations; drought- deciduousness can reduce vulnerability to drought; phenology of evergreens needs more investigation.
2) Plant Hydraulics	Interactions between hydraulic failure (e.g. low soil moisture availability) and C limitation (e.g. stomatal closure) during drought should be included in models. Account for turgor loss, hydraulic failure traits, costs to recover damaged xylem.
3) Dynamic Carbon Allocation	C allocation based on eco-evolutionary optimality (EEO) and allometric partitioning theory in addition to, or replacing ratio-based optimal partitioning theory, and fixed allocation ratios. Explore root allocation that could offset soil water deficits.
4) Non-structural Carbohydrate (NSC) Storage	Deciding best practices for NSC representation in models. Better understanding of NSC storage required to mitigate plant mortality during C starvation and interactions with avoiding hydraulic failure during severe droughts.
<b>States Variables</b>	
1) Plant-Soil Water Availability	Better quantification of the amount and accessibility of plant-available water for surviving trees, and tradeoff between increased structural productivity but vulnerability to subsequent droughts. Future relevance, or benefit, of lower water demand due to thinning with UCEs.
2) Plant Functional Diversity	Understand how higher diversity of plant physiological traits and drought-resistance strategies will enhance community resistance to drought; models still need to account for shifts in diverse functionality, including deciduousness shifts and interplay of regrowth structural overshoot followed by amplified mortality from hotter UCEs.
3) Stand Demography	Large trees more vulnerable to drought; need data on changes in C stock with UCEs in high-density smaller tree stands vs. stands with larger trees. Using ‘self-organization’ principles for modeling stand level competition and coexistence under UCEs.

873





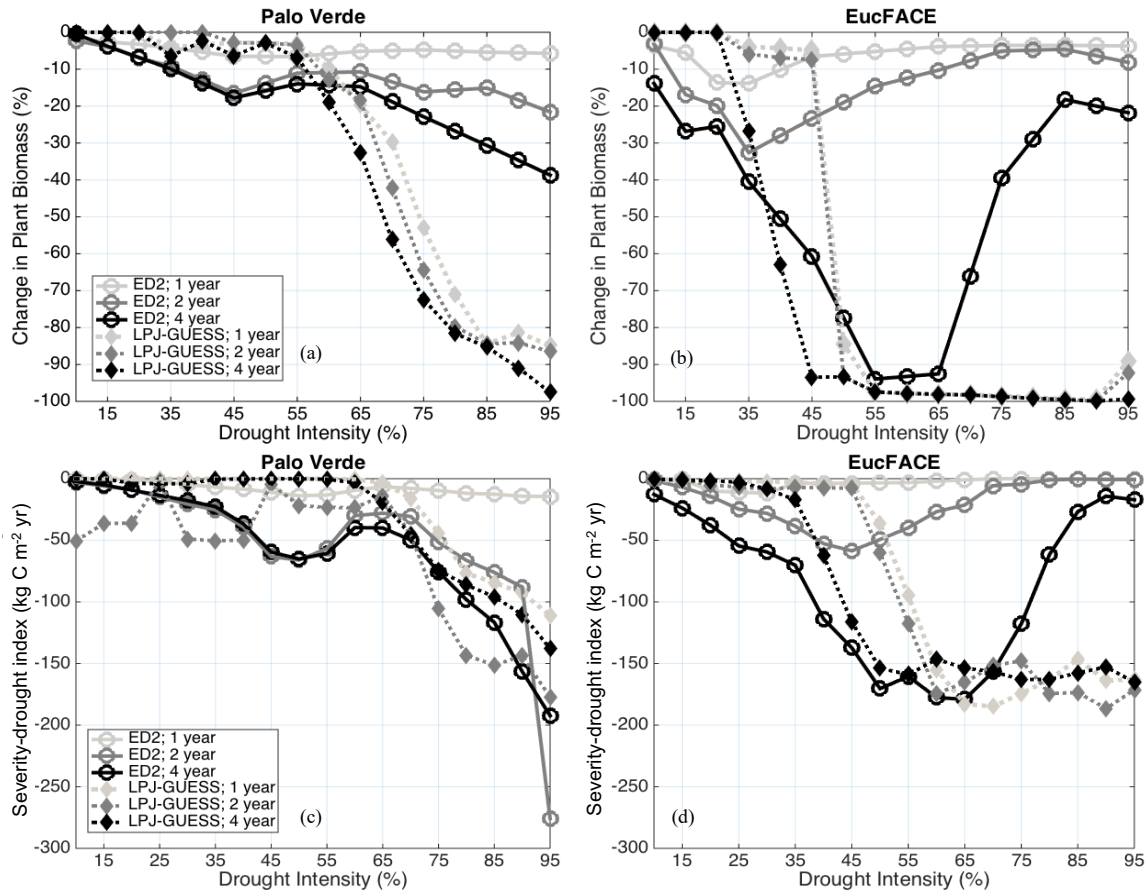
875

876 **Figure 1** Conceptual diagrams showing impacts of extreme droughts (unprecedented climate  
 877 extremes, UCEs; i.e., record-breaking droughts) on plant C stocks. (a) **Conceptual diagram of**  
 878 **UCE C loss:** potential loss in C stock as a function of increasing drought intensity (0-100%  
 879 precipitation removal) and drought duration (1, 2 or 4 years of drought). In this example, an  
 880 arbitrary threshold of 45% precipitation reduction and 4-year drought duration is assumed to  
 881 correspond to a UCE. Hypotheses include nonlinear and threshold responses to drought intensity  
 882 (H1a), drought duration via different slope responses (H1b), and combined effects of both  
 883 drought intensity and durations (H1c). (b) **Conceptualized diagram of integrated C change:**  
 884 responses of forest C stocks to a large (grey) and small (black) UCE. “Severity-drought index”  
 885 (kg C m<sup>-2</sup> yr) denotes the integral of the C loss over time and is calculated from the two arrows:  
 886 the total loss in C (kg C m<sup>-2</sup>) due to drought, and the time (yr) to recover 50% of the pre-drought  
 887 C stock. (c) **Conceptualized UCE-climate C change diagram:** hypothetical response in  
 888 terrestrial “severity-climate index” (kg C m<sup>-2</sup> yr) due to eCO<sub>2</sub> (blue line), rising temperature (red  
 889 line), interaction between eCO<sub>2</sub> and temperature (dashed purple), and combined interactions

890 among eCO<sub>2</sub>, temperature, and UCEs of prolonged durations (green line), all relative to a  
891 reference drought of normal duration with no warming (black line). Severity-climate index  
892 denotes the difference in severity-drought index (see panel b) between a scenario of changing  
893 climatic drivers and the reference drought with no climate change (control). (d) **Conceptual**  
894 **UCE amplification diagram:** hypothetical amplified change in forest C stocks to eCO<sub>2</sub> and  
895 temperature relative to the pre-warming historical past (based on Jump et al. (2017)). Change in  
896 C stock greater than zero indicates a ‘structural overshoot’ (SO) due to favorable environmental  
897 conditions and/or recovery from an extreme drought-heat event (EE). Hashed black areas  
898 indicate a structural overshoot due to eCO<sub>2</sub>, which occurs over the historical CO<sub>2</sub> levels (dashed  
899 blue line). Initially, an eCO<sub>2</sub> effect leads to a larger increase in structural overshoot (due to CO<sub>2</sub>  
900 fertilization), driving more extreme vegetation mortality (‘mortality overshoot’ - MO) relative to  
901 historical dieback events and thus a greater decrease in C stock. Increased warming through time  
902 increasingly counteracts any CO<sub>2</sub> fertilization effect. While the amplitude of post-UCE C stock  
903 recoveries remains large, net C stock values eventually decline (downward curvature, and  
904 widening of the red shaded area) due to more pronounced loss in C stocks (and greater  
905 ecosystem state change) from hotter UCEs and longer recovery periods. We conceptualize how  
906 oscillations between SOs and MOs could be amplified and the widening of the shaded areas  
907 represents increased variability in how unprecedented eCO<sub>2</sub> levels and temperatures will affect  
908 ecosystems in the future compared to historical.

909 SO = structural overshoot, MO = mortality overshoot, EE = historically extreme drought-heat  
910 event, UCE = unprecedented climate extreme.

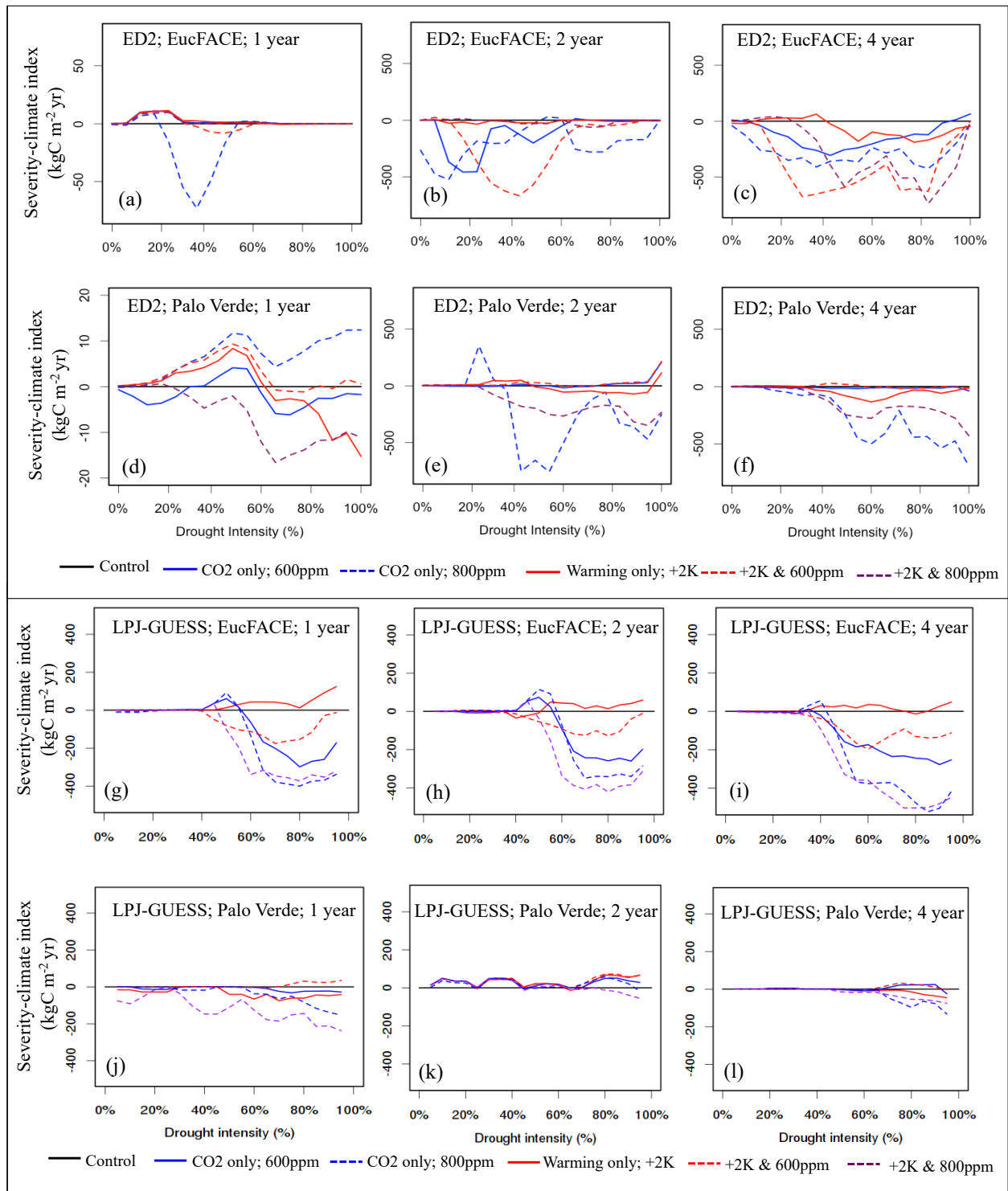
911



912

913 **Figure 2** Modeled change in biomass (%) at the end of drought periods of different lengths (1, 2,  
 914 and 4-year droughts) and intensities (up to 95% precipitation removed) at (a) Palo Verde, and (b)  
 915 EucFACE, for the ED2 and LPJ-GUESS models. Modeled severity-drought index (C reduction  
 916 due to extreme drought integrated over time until biomass recovers to 50% of the non-drought  
 917 baseline biomass) at (c) Palo Verde and (d) EucFACE.

918



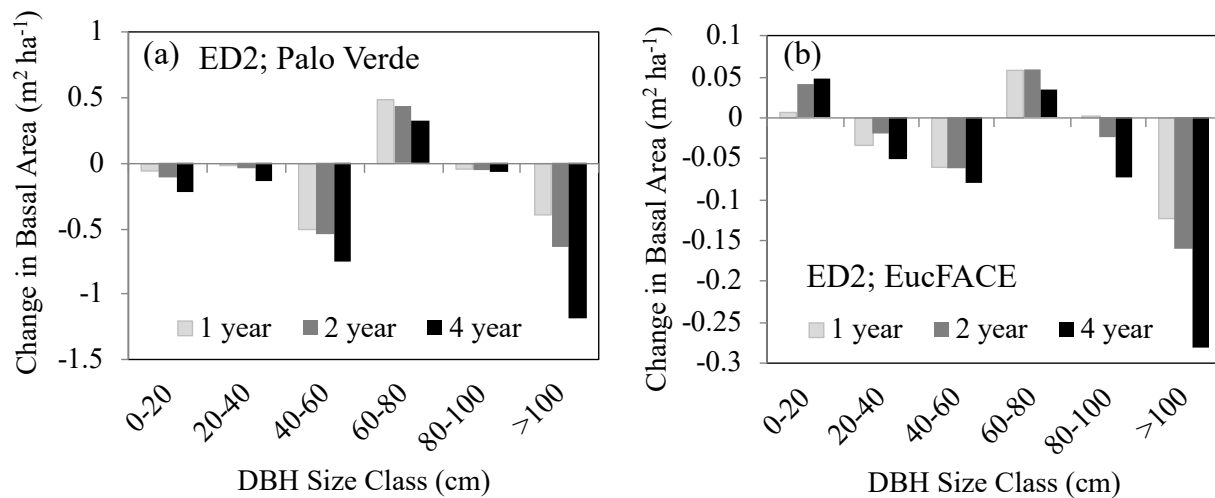
919

920 **Figure 3** Vegetation C response to interactions between drought intensity (0% to 100%  
 921 precipitation reduction), drought durations (1, 2, 4-year droughts), and idealized scenarios of  
 922 warming and eCO<sub>2</sub> compared to the control simulation, simulated by two VDMs; ED2 (a-f) and  
 923 LPJ-GUESS (g-l) at two sites (EucFACE and Palo Verde). The scenarios include a control

924 (current temperature; 400 ppm atmospheric CO<sub>2</sub>), two eCO<sub>2</sub> scenarios (600 ppm or 800 ppm),  
 925 elevated temperature (2 K above current), and a combination of eCO<sub>2</sub> (600 ppm or 800 ppm) and  
 926 higher temperature. Vegetation response is quantified as “severity-climate index” (in kg C m<sup>-2</sup>  
 927 yr; Eq. 4), which is defined as the difference between severity-drought index (i.e., carbon loss  
 928 due to only drought) and a given scenario of drought plus change in climatic drivers, relative to  
 929 the control (i.e., no climate change). Negative values for severity-climate index indicate that  
 930 warming and/or eCO<sub>2</sub> leads to stronger C losses and/or longer recovery, while positive values for  
 931 severity-climate index indicates a buffering effect.

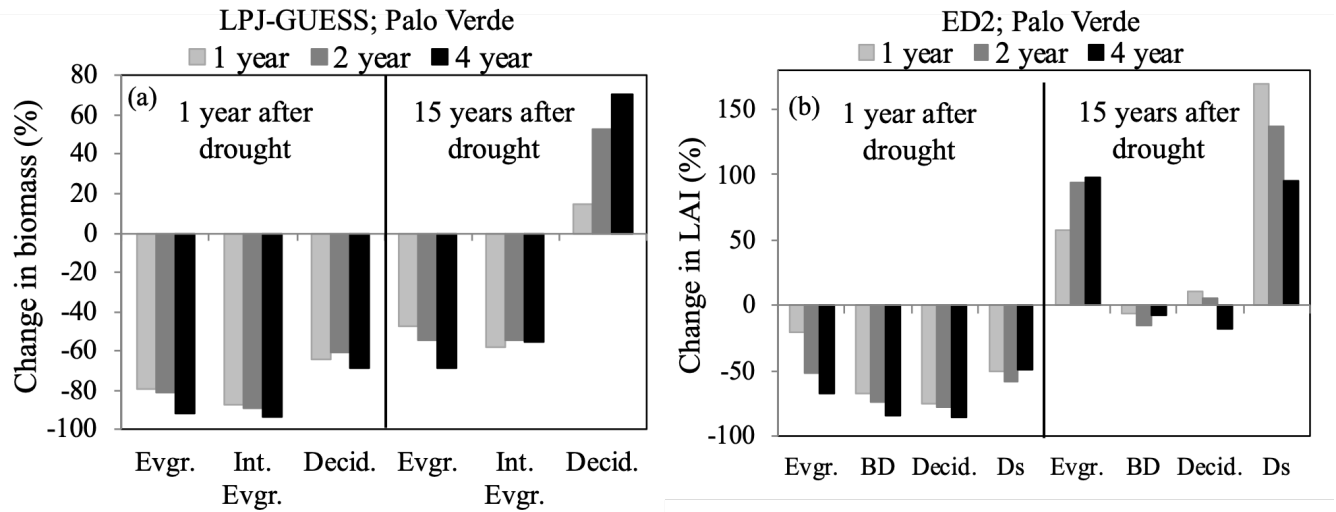
932

933



934

935 **Figure 4** Change in basal area (m<sup>2</sup> ha<sup>-1</sup>) immediately following either 1, 2, or 4 year droughts for  
 936 six increasing size class bins (DBH, cm) as predicted by the ED2 model for (a) the Palo Verde  
 937 site, with 90% precipitation removed, and (b) the EucFACE site with 50% precipitation  
 938 removed.



940

941

942 **Figure 5** Percent change in community composition, represented by plant functional type (PFT),

943 the year following three drought durations of UCEs (1, 2, and 4-year droughts and 90%

944 precipitation removed) as well as 15 years after droughts, for the tropical Palo Verde site by (a)

945 LPJ-GUESS reported in biomass change, and (b) ED2 reported in LAI change. Even though Ds

946 had the strongest recovery, it should be noted it was the least abundant PFT at this site. Evgr. =

947 evergreen, Int. Ever. = intermediate evergreen, Decid. = deciduous, BD = brevi-deciduous, Ds =

948 deciduous stem-succulent. EucFACE data not shown because only one PFT present (evergreen

949 tree).

950 References:

951

952 Adams, H.D., Guardiola-Claramonte, M., Barron-Gafford, G.A., Villegas, J.C., Breshears, D.D.,  
953 Zou, C.B. et al.: Temperature sensitivity of drought-induced tree mortality portends  
954 increased regional die-off under global-change-type drought, *PNAS*, 106, 7063-7066, 2009.

955 Adams, H.D., Barron-Gafford, G.A., Minor, R.L., Gardea, A.A., Bentley, L.P., Law, D.J. et al.:  
956 Temperature response surfaces for mortality risk of tree species with future drought,  
957 *Environ. Res. Lett.*, 12, 115014, 2017a.

958 Adams, H.D., Zeppel, M.J.B., Anderegg, W.R.L., Hartmann, H., Landhäusser, S.M., Tissue, D.T.  
959 et al.: A multi-species synthesis of physiological mechanisms in drought-induced tree  
960 mortality, *Nature Ecol. & Evol.*, 1, 1285-1291, 2017b.

961 Aguirre, BA, Hsieh, B, Watson, SJ, Wright, AJ.: The experimental manipulation of atmospheric  
962 drought: Teasing out the role of microclimate in biodiversity experiments, *J. Ecol.*, 109,  
963 1986– 1999, <https://doi.org/10.1111/1365-2745.13595>, 2021.

964 Ahlström, A., Schurgers, G., Arneth, A., and Smith, B.: Robustness and uncertainty in terrestrial  
965 ecosystem carbon response to CMIP5 climate change projections, *Environ. Res. Lett.*, 7,  
966 044008, 2012.

967 Ainsworth, E.A., and Long, S.P.: What have we learned from 15 years of free-air CO<sub>2</sub>  
968 enrichment (FACE)? A meta-analytic review of the responses of photosynthesis, canopy  
969 properties and plant production to rising CO<sub>2</sub>, *New Phytol.*, 165, 351-372, 2005.

970 Allen, C.D., Breshears, D.D., and McDowell, N.G.: On underestimation of global vulnerability to  
971 tree mortality and forest die-off from hotter drought in the Anthropocene, *Ecosphere*, 6,  
972 art129, 2015.

973 Allen, K., Dupuy, J.M., Gei, M.G., Hulshof, C.M., Medvigy, D., Pizano, C. et al.: Will seasonally  
974 dry tropical forests be sensitive or resistant to future changes in 558 rainfall regimes?  
975 *Environ. Res. Lett.*, 12, 023001, 2017.

976 Amiro, B.D., Barr, A.G., Barr, J.G., Black, T.A., Bracho, R., Brown, M. et al.: Ecosystem carbon  
977 dioxide fluxes after disturbance in forests of North America, *J. Geophys. Res.*  
978 *Biogeosciences*, 115, 2010.

979 Anderegg, W.R.L., Hicke, J.A., Fisher, R.A., Allen, C.D., Aukema, J., Bentz, B. et al.: Tree  
980 mortality from drought, insects, and their interactions in a changing climate, *New Phytol.*,  
981 208, 674-683, 2015.

982 Anderegg, W.R.L., Klein, T., Bartlett, M., Sack, L., Pellegrini, A.F.A., Choat, B. et al.: Meta-  
983 analysis reveals that hydraulic traits explain cross-species patterns of drought-induced tree  
984 mortality across the globe, *PNAS*, 113, 5024-5029, 2016a.

985 Anderegg, W.R.L., Martinez-Vilalta, J., Cailleret, M., Camarero, J.J., Ewers, B.E., Galbraith, D.  
986 et al.: When a Tree Dies in the Forest: Scaling Climate-Driven Tree Mortality to Ecosystem  
987 Water and Carbon Fluxes, *Ecosystems*, 19, 1133-1147, 2016b.

988 Anderegg, W.R.L., Konings, A.G., Trugman, A.T., Yu, K., Bowling, D.R., Gabbitas, R. et al.:  
989 Hydraulic diversity of forests regulates ecosystem resilience during drought, *Nature*, 561,  
990 538-541, 2018.

991 Anderegg, W.R.L. and Venturas, M.D.: Plant hydraulics play a critical role in Earth system  
992 fluxes, *New Phytol*, 226, 1535-1538, <https://doi.org/10.1111/nph.16548>, 2020.

993 Asner, G.P., Brodrick, P.G., Anderson, C.B., Vaughn, N., Knapp, D.E., and Martin, R.E.:  
994 Progressive forest canopy water loss during the 2012–2015 California drought. *PNAS*, 113,  
995 E249-E255, 2016.

996 Arora, V.K., Katavouta, A., Williams, R.G., Jones, C.D., Brovkin, V., Friedlingstein, P., et al.:  
997 Carbon-concentration and carbon-climate feedbacks in CMIP6 models and their  
998 comparison to CMIP5 models, *Biogeosciences*, 17, 4173–4222, 2020.

999 Bai, Y., Wu, J., Xing, Q., Pan, Q., Huang, J., Yang, D. et al.: PRIMARY PRODUCTION AND  
1000 RAIN USE EFFICIENCY ACROSS A PRECIPITATION GRADIENT ON THE  
1001 MONGOLIA PLATEAU, *Ecology*, 89, 2140-2153, 2008.

1002 Beier, C., Beierkuhnlein, C., Wohlgemuth, T., Penuelas, J., Emmett, B., Körner, C. et al.:  
1003 Precipitation manipulation experiments – challenges and recommendations for the future,  
1004 *Ecol. Lett.*, 15, 899-911, 2012.

1005 Bennett, A.C., McDowell, N.G., Allen, C.D., and Anderson-Teixeira, K.J.: Larger trees suffer  
1006 most during drought in forests worldwide, *Nature Plants*, 1, 15139, 2015.

1007 Biederman, J.A., Meixner, T., Harpold, A.A., Reed, D.E., Gutmann, E.D., Gaun, J.A. et al.:  
1008 Riparian zones attenuate nitrogen loss following bark beetle-induced lodgepole pine  
1009 mortality, *J. Geophys. Res. Biogeosciences*, 121, 933-948, 2016.

1010 Biederman, J.A., Somor, A.J., Harpold, A.A., Gutmann, E.D., Breshears, D.D., Troch, P.A. et al.:  
1011 Recent tree die-off has little effect on streamflow in contrast to expected increases from  
1012 historical studies, *Water Resources Res.*, 51, 9775-9789, 2015.

1013 Blyth, E.M., Arora, V.K., Clark, D.B. et al.: Advances in Land Surface Modelling, *Curr. Clim.*  
1014 *Change Rep.*, 7, 45–71, <https://doi.org/10.1007/s40641-021-00171-5>, 2021.

1015 Borchert, R., Rivera, G., and Hagnauer, W.: Modification of Vegetative Phenology in a Tropical  
1016 Semi-deciduous Forest by Abnormal Drought and Rain, *Biotropica*, 34, 27-39, 2002.

1017 Bonan, G.: Vegetation Demography, in: *Climate Change and Terrestrial Ecosystem Modeling*,  
1018 Cambridge: Cambridge University Press, 344-364, doi:10.1017/9781107339217.020, 2019.

1019 Bonan, G. B., Patton, E. G., Finnigan, J. J., Baldocchi, D. D., and Harman, I. N.: Moving beyond  
1020 the incorrect but useful paradigm: reevaluating big-leaf and multilayer plant canopies to  
1021 model biosphere-atmosphere fluxes – a review, *Agr. Forest Meteorol.*, 306,  
1022 108435, <https://doi.org/10.1016/j.agrformet.2021.108435>, 2021.

1023 Brando, P.M., Paolucci, L., Ummenhofer, C.C., Ordway, E.M., Hartmann, H., Cattau, M.E.,  
1024 Rattis, L., Medjibe, V., Coe, M.T., Balch, J.: Droughts, Wildfires, and Forest Carbon  
1025 Cycling: A Pantropical Synthesis, *Annual Review of Earth and Planetary Sciences*, 47, 555-  
1026 581, 2019.

1027 Breshears, D.D., Myers, O.B., Meyer, C.W., Barnes, F.J., Zou, C.B., Allen, C.D. et al.: Tree die-  
1028 off in response to global change-type drought: mortality insights from a decade of plant  
1029 water potential measurements, *Front. Ecol. Environ.*, 7, 185-189, 2009.

1030 Brodribb, T.J., Bowman, D.J.M.S., Nichols, S., Delzon, S. and Burlett, R.: Xylem function and  
1031 growth rate interact to determine recovery rates after exposure to extreme water deficit, *New*  
1032 *Phytol.*, 188, 533-542, 2010.

1033 Bugmann, H., and Seidl, R.: The evolution, complexity and diversity of models of long-term  
1034 forest dynamics. *J. of Ecol.*, 110, 2288– 2307, <https://doi.org/10.1111/1365-2745.13989>,  
1035 2022.

1036 Carreño-Rocabado, G., Peña-Claros, M., Bongers, F., Alarcón, A., Licona, J.-C., and Poorter, L.:  
1037 Effects of disturbance intensity on species and functional diversity in a tropical forest, *J.*  
1038 *Ecology*, 100, 1453-1463, 2012.

1039 Chapman, T.B., Veblen, T.T., and Schoennagel, T.: Spatiotemporal patterns of mountain pine  
1040 beetle activity in the southern Rocky Mountains, *Ecology*, 93, 2175-2185, 2012.



1041 Chiang, F., Mazdiyasn, O., and AghaKouchak, A.: Evidence of anthropogenic impacts on global  
1042 drought frequency, duration, and intensity, *Nat Commun.*, 12, 2754,  
1043 <https://doi.org/10.1038/s41467-021-22314-w>, 2021.

1044 Choat, B., Brodribb, T.J., Brodersen, C.R., Duursma, R.A., López, R., and Medlyn, B.E.: Triggers  
1045 of tree mortality under drought, *Nature*, 558, 531-539, 2018.

1046 Choat, B., Jansen, S., Brodribb, T.J., Cochard, H., Delzon, S., Bhaskar, R. et al.: Global  
1047 convergence in the vulnerability of forests to drought, *Nature*, 491, 752-755, 2012.

1048 Christoffersen, B.O., Gloor, M., Fauset, S., Fyllas, N.M., Galbraith, D.R., Baker, T.R. et al.:  
1049 Linking hydraulic traits to tropical forest function in a size-structured and trait-driven model  
1050 (TFS v.1-Hydro), *Geosci. Model Dev. Discuss.*, 2016, 1-60, 2016.

1051 Ciais, P., Reichstein, M., Viovy, N., Granier, A., Ogée, J., Allard, V. et al.: Europe-wide  
1052 reduction in primary productivity caused by the heat and drought in 2003, *Nature*, 437, 529,  
1053 2005.

1054 Clark, K.L., Skowronski, N., and Hom, J.: Invasive insects impact forest carbon dynamics, *Glob.*  
1055 *Change Biol.*, 16, 88-101, 2010.

1056 Coley, P., Massa, M., Lovelock, C., Winter, K.: Effects of elevated CO<sub>2</sub> on foliar chemistry of  
1057 saplings of nine species of tropical tree, *Oecologia*, 2002.

1058 Creeden, E.P., Hicke, J.A., and Buotte, P.C.: Climate, weather, and recent mountain pine beetle  
1059 outbreaks in the western United States, *Forest Ecol. Manag.*, 312, 239-251, 2014.

1060 D'Amato, A.W., Bradford, J.B., Fraver, S. and Palik, B.J.: Effects of thinning on drought  
1061 vulnerability and climate response in north temperate forest ecosystems, *Eco. Applications*,  
1062 23, 1735-1742, 2013.

1063 da Costa, A.C.L., Galbraith, D., Almeida, S., Portela, B.T.T., da Costa, M., de Athaydes Silva  
1064 Junior, J. et al., Effect of 7 yr of experimental drought on vegetation dynamics and biomass  
1065 storage of an eastern Amazonian rainforest, *New Phytol.*, 187, 579-591, 2010.

1066 De Kauwe, M.G., Medlyn, B.E., Zaehle, S., Walker, A.P., Dietze, M.C., Wang, Y.-P. et al.:  
1067 Where does the carbon go? A model-data intercomparison of vegetation carbon allocation  
1068 and turnover processes at two temperate forest free-air CO<sub>2</sub> enrichment sites, *New Phytol.*,  
1069 203, 883-899, 2014.

1070 Dietze, M.C., and Matthes, J.H.: A general ecophysiological framework for modelling the impact  
1071 of pests and pathogens on forest ecosystems, *Ecol. Lett.*, 17, 1418-1426, 2014.

1072 Döscher, R., Acosta, M., et al.: The EC-Earth3 Earth System Model for the Climate Model  
1073 Intercomparison Project 6, *Geosci. Model Dev. Discuss.* [preprint],  
1074 <https://doi.org/10.5194/gmd-2020-446>, in revision, 2022.

1075 Dreesen, F.E., De Boeck, H.J., Janssens, I.A., and Nijs, I.: Do successive climate extremes  
1076 weaken the resistance of plant communities? An experimental study using plant  
1077 assemblages, *Biogeosciences*, 11, 109-121, 2014.

1078 Eamus, D., Boulain, N., Cleverly, J., and Breshears, D.D.: Global change-type drought-induced  
1079 tree mortality: vapor pressure deficit is more important than temperature per se in causing  
1080 decline in tree health, *Ecol. Evol.*, 3, 2711-2729, 2013.

1081 Eller, C.B., Rowland, L., Mencuccini, M., Rosas, T., Williams, K., Harper, A. et al.: Stomatal  
1082 optimization based on xylem hydraulics (SOX) improves land surface model simulation of  
1083 vegetation responses to climate, *New Phytol.*, 226, 1622-  
1084 1637, <https://doi.org/10.1111/nph.16419>, 2020.

1085 Ellsworth, David S., Anderson, Ian C., Crous, Kristine Y., Cooke, J., Drake, John E., Gherlenda,  
1086 Andrew N. et al.: Elevated CO<sub>2</sub> does not increase eucalypt forest productivity on a low-  
1087 phosphorus soil, *Nature Climate Change*, 7, 279, 2017.

1088 ENQUIST, B.J., and ENQUIST, C.A.F.: Long-term change within a Neotropical forest: assessing  
1089 differential functional and floristic responses to disturbance and drought, *Glob. Change*  
1090 *Biol.*, 17, 1408-1424, 2011.

1091 Esquivel-Muelbert, A., Baker, T.R., Dexter, K.G., Lewis, S.L., Brienen, R.J.W., Feldpausch, T.R.  
1092 et al.: Compositional response of Amazon forests to climate change, *Glob. Change Biol.*, 25,  
1093 39-56, 2019.

1094 Eziz, A., Yan, Z., Tian, D., Han, W., Tang, Z., and Fang, J.: Drought effect on plant biomass  
1095 allocation: A meta-analysis, *Ecol. Evol.*, 7, 11002-11010, 2017.

1096 Fang, Y., Leung, L. R., Knox, R., Koven, C., and Bond-Lamberty, B.: Impact of the numerical  
1097 solution approach of a plant hydrodynamic model (v0.1) on vegetation dynamics, *Geosci.*  
1098 *Model Dev.*, 15, 6385–6398, <https://doi.org/10.5194/gmd-15-6385-2022>, 2022.

1099 Feldpausch, T.R., Phillips, O.L., Brienen, R.J.W., Gloor, E., Lloyd, J., Lopez-Gonzalez, G. et al.:  
1100 Amazon forest response to repeated droughts, *Global Biogeochemical Cycles*, 30, 964-982,  
1101 2016.

1102 Fisher, R.A., Muszala, S., Verstein, M., Lawrence, P., Xu, C., McDowell, N.G. et al.: Taking  
1103 off the training wheels: the properties of a dynamic vegetation model without climate  
1104 envelopes, *CLM4.5(ED)*, *Geosci. Model Dev.*, 8, 3593-3619, 2015.

1105 Fisher, R.A., Koven, C.D., Anderegg, W.R.L., Christoffersen, B.O., Dietze, M.C., Farrior, C.E. et  
1106 al.: Vegetation demographics in Earth System Models: A review of progress and priorities,  
1107 *Glob. Change Biol.*, 24, 35-54, 2018.

1108 Fisher, R. A., and Koven, C. D.: Perspectives on the future of land surface models and the  
1109 challenges of representing complex terrestrial systems, *JAMES*, 12,  
1110 e2018MS001453, <https://doi.org/10.1029/2018MS001453>, 2020.

1111 Fleischer, K., Rammig, A., De Kauwe, M.G., Walker, A.P., Domingues, T.F., Fuchslueger, L. et  
1112 al.: Amazon forest response to CO<sub>2</sub> fertilization dependent on plant phosphorus acquisition,  
1113 *Nature Geoscience*, 12, 736-741, 2019.

1114 Frank, D., Reichstein, M., Bahn, M., Thonicke, K., Frank, D., Mahecha, M.D. et al.: Effects of  
1115 climate extremes on the terrestrial carbon cycle: concepts, processes and potential future  
1116 impacts, *Glob. Change Biol.*, 21, 2861-2880, 2015.

1117 Franklin, O., McMurtrie, R.E., Iversen, C.M., Crous, K.Y., Finzi, A.C., Tissue, D.T., Ellsworth,  
1118 D.S., Oren, R. Norby, R.J.: Forest fine-root production and nitrogen use under elevated  
1119 CO<sub>2</sub>: contrasting responses in evergreen and deciduous trees explained by a common  
1120 principle, *Glob. Change Biol.*, 15, 132-144, 2009.

1121 Franklin, O., Johansson, J., Dewar, R.C., Dieckmann, U., McMurtrie, R.E., Brännström, Å.,  
1122 Dybzinski, R.: Modeling carbon allocation in trees: a search for principles, *Tree Physiology*,  
1123 32, 648–666, <https://doi.org/10.1093/treephys/tpr138>, 2012.

1124 Franklin, O., Harrison, S.P., Dewar, R. et al.: Organizing principles for vegetation dynamics. *Nat.*  
1125 *Plants*, 6, 444–453, <https://doi.org/10.1038/s41477-020-0655-x>, 2020.

1126 Friend, A.D., Lucht, W., Rademacher, T.T., Keribin, R., Betts, R., Cadule, P. et al.: Carbon  
1127 residence time dominates uncertainty in terrestrial vegetation responses to future climate  
1128 and atmospheric CO<sub>2</sub>, *PNAS*, 111, 3280-3285, 2014.

1129 Gerten, D., LUO, Y., Le MAIRE, G., PARTON, W.J., KEOUGH, C., WENG, E. et al.: Modelled  
1130 effects of precipitation on ecosystem carbon and water dynamics in different climatic zones,  
1131 *Glob. Change Biol.*, 14, 2365-2379, 2008.

1132 Goulden, M.L., and Bales, R.C.: California forest die-off linked to multi-year deep soil drying in  
1133 2012–2015 drought, *Nature Geoscience*, 12, 632-637, 2019.

1134 Gray, S.B., Dermody, O., Klein, S.P., Locke, A.M., McGrath, J.M., Paul, R.E. et al.: Intensifying  
1135 drought eliminates the expected benefits of elevated carbon dioxide for soybean, *Nature*  
1136 *Plants*, 2, 16132, 2016.

1137 Greenwood, S., Ruiz-Benito, P., Martínez-Vilalta, J., Lloret, F., Kitzberger, T., Allen, C.D. et al.:  
1138 Tree mortality across biomes is promoted by drought intensity, lower wood density and  
1139 higher specific leaf area, *Ecol. Lett.*, 20, 539-553, 2017.

1140 Griffin, D., and Anchukaitis, K.J.: How unusual is the 2012–2014 California drought? *Geophys.*  
1141 *Res. Lett.*, 41, 9017-9023, 2014.

1142 Hanbury-Brown, A.R., Powell, T.L., Muller-Landau, H.C., Wright, S.J. and Kueppers, L.M.:  
1143 Simulating environmentally-sensitive tree recruitment in vegetation demographic models,  
1144 *New Phytol.*, 235, 78-93, <https://doi.org/10.1111/nph.18059>, 2022.

1145 Harrison, S.P., Cramer, W., Franklin, O., Prentice, I.C., Wang, H., Brännström, Å., et al.: Eco-  
1146 evolutionary optimality as a means to improve vegetation and land-surface models, *New*  
1147 *Phytol.*, 231, 2125-2141, <https://doi.org/10.1111/nph.17558>, 2021.

1148 Hickler, T., Smith, B., Sykes, M.T., Davis, M.B., Sugita, S., and Walker, K.: USING A  
1149 GENERALIZED VEGETATION MODEL TO SIMULATE VEGETATION DYNAMICS  
1150 IN NORTHEASTERN USA, *Ecology*, 85, 519-530, 2004.

1151 Holm, J. A., Knox, R. G., Zhu, Q., Fisher, R. A., Koven, C. D., Nogueira Lima, A. J., et al.: The  
1152 central Amazon biomass sink under current and future atmospheric CO<sub>2</sub>: Predictions from  
1153 big-leaf and demographic vegetation models, *J. Geophys. Res. Biogeosciences*, 125,  
1154 e2019JG005500. <https://doi.org/10.1029/2019JG005500>, 2020.

1155 Hovenden, M.J., Newton, P.C.D., and Wills, K.E.: Seasonal not annual rainfall determines  
1156 grassland biomass response to carbon dioxide, *Nature*, 511, 583, 2014.

1157 Hubbard, R.M., Rhoades, C.C., Elder, K., and Negron, J.: Changes in transpiration and foliage  
1158 growth in lodgepole pine trees following mountain pine beetle attack and mechanical  
1159 girdling, *Forest Ecol. Manag.*, 289, 312-317, 2013.

1160 IPCC: Managing the Risks of Extreme Events and Disasters to Advance Climate Change  
1161 Adaptation. A Special Report of Working Groups I and II of the Intergovernmental Panel on  
1162 Climate Change. (ed. Field, C.B., V. Barros, T.F. Stocker, D. Qin, D.J. Dokken, K.L. Ebi,  
1163 M.D. Mastrandrea, K.J. Mach, G.-K. Plattner, S.K. Allen, M. Tignor, and P.M. Midgley)  
1164 Cambridge, UK, and New York, NY, USA, p. 582 pp, 2012.

1165 IPCC: Climate Change 2021: The Physical Science Basis. Contribution of Working Group I to the  
1166 Sixth Assessment Report of the Intergovernmental Panel on Climate Change [Masson-  
1167 Delmotte, V., P. Zhai, A. Pirani, S.L. Connors, C. Péan, S. Berger, N. Caud, Y. Chen, L.  
1168 Goldfarb, M.I. Gomis, M. Huang, K. Leitzell, E. Lonnoy, J.B.R. Matthews, T.K. Maycock,  
1169 T. Waterfield, O. Yelekçi, R. Yu, and B. Zhou (eds.)]. Cambridge University Press, 2021.

1170 Jiang, M., Medlyn, B.E., Drake, J.E., Duursma, R.A., Anderson, I.C., Barton, C.V.M., Boer,  
1171 M.B., Carrillo, Y., Castañeda-Gómez, L., Collins, L., et al.: The fate of carbon in a mature  
1172 forest under carbon dioxide enrichment, *Nature*, 580, 227-231,  
1173 <https://doi.org/10.1038/s41586-020-2128-9>, 2020.

1174 Joslin, J.D., Wolfe, M.H., and Hanson, P.J.: Effects of altered water regimes on forest root  
1175 systems, *New Phytol.*, 147, 117-129, 2000.

1176 Jump, A.S., Ruiz-Benito, P., Greenwood, S., Allen, C.D., Kitzberger, T., Fensham, R. et al.:  
1177 Structural overshoot of tree growth with climate variability and the global spectrum of  
1178 drought-induced forest dieback, *Glob. Change Biol.*, 23, 3742-3757, 2017.

1179 Kalacska, M.E.R., Sánchez-Azofeifa, G.A., Calvo-Alvarado, J.C., Rivard, B. and Quesada, M.:  
1180 Effects of Season and Successional Stage on Leaf Area Index and Spectral Vegetation  
1181 Indices in Three Mesoamerican Tropical Dry Forests, *Biotropica*, 37, 486-  
1182 496, <https://doi.org/10.1111/j.1744-7429.2005.00067.x>, 2005.

1183 Kannenberg, S.A., Schwalm, C.R. and Anderegg, W.R.L.: Ghosts of the past: how drought legacy  
1184 effects shape forest functioning and carbon cycling, *Ecol. Lett.*, 23: 891-901,  
1185 <https://doi.org/10.1111/ele.13485>, 2020.

1186 Kattge, J., DÍAZ, S., LAVOREL, S., PRENTICE, I.C., LEADLEY, P., BÖNISCH, G. et al.: TRY  
1187 – a global database of plant traits, *Global Change Biol*, 17, 2905-2935, 2011.

1188 Kayler, Z.E., De Boeck, H.J., Fatichi, S., Grünzweig, J.M., Merbold, L., Beier, C. et al.:  
1189 Experiments to confront the environmental extremes of climate change, *Front. Ecol.*  
1190 *Environ.*, 13, 219-225, 2015.

1191 Keenan, T.F., Hollinger, D.Y., Bohrer, G., Dragoni, D., Munger, J.W., Schmid, H.P. et al.:  
1192 Increase in forest water-use efficiency as atmospheric carbon dioxide concentrations rise,  
1193 *Nature*, 499, 324-327, 2013.

1194 Kennedy, D., Swenson, S., Oleson, K. W., Lawrence, D. M., Fisher, R., Lola da Costa, A. C., and  
1195 Gentine, P.: Implementing plant hydraulics in the Community Land Model, version 5,  
1196 *JAMES*, 11, 485– 513, <https://doi.org/10.1029/2018MS001500>, 2019.

1197 Li, L., Yang, Z.-L., Matheny, A. M., Zheng, H., Swenson, S. C., Lawrence, D. M., et  
1198 al.: Representation of plant hydraulics in the Noah-MP land surface model: Model  
1199 development and multiscale evaluation, *JAMES*, 13,  
1200 e2020MS002214, <https://doi.org/10.1029/2020MS002214>, 2021.

1201 Li, Q., Lu, X., Wang, Y., Huang, X., Cox, P. M., and Luo, Y.: Leaf area index identified as a  
1202 major source of variability in modeled CO<sub>2</sub> fertilization, *Biogeosciences*, 15, 6909–6925,  
1203 <https://doi.org/10.5194/bg-15-6909-2018>, 2018.

1204 Liu, Y., Parolari, A.J., Kumar, M., Huang, C.-W., Katul, G.G., and Porporato, A.: Increasing  
1205 atmospheric humidity and CO<sub>2</sub> concentration alleviate forest mortality risk, *PNAS*, 114,  
1206 9918-9923, 2017.

1207 Lloret, F., Escudero, A., Iriondo, J.M., Martínez-Vilalta, J., and Valladares, F.: Extreme climatic  
1208 events and vegetation: the role of stabilizing processes, *Glob. Change Biol.*, 18, 797-805,  
1209 2012.

1210 Luo, Y., Gerten, D., Le Maire, G., Parton, W.J., Weng, E., Zhou, X. et al.: Modeled interactive  
1211 effects of precipitation, temperature, and [CO<sub>2</sub>] on ecosystem carbon and water dynamics in  
1212 different climatic zones, *Glob. Change Biol.*, 14, 1986-1999, 2008.

1213 Luo, Y.Q., Randerson, J.T., Abramowitz, G., Bacour, C., Blyth, E., Carvalhais, N. et al.: A  
1214 framework for benchmarking land models, *Biogeosciences*, 9, 3857-3874, 2012.

1215 Luo, Y., Jiang, L., Niu, S., Zhou, X.: Nonlinear responses of land ecosystems to variation in  
1216 precipitation, *New Phytol.*, 214, 5–7, 2017.

1217 Ma, W., Zhai, L., Pivovarov, A., Shuman, J., Buotte, P., Ding, J., Christoffersen, B., Knox, R.,  
1218 Moritz, M., Fisher, R. A., Koven, C. D., Kueppers, L., and Xu, C.: Assessing climate

1219 change impacts on live fuel moisture and wildfire risk using a hydrodynamic vegetation  
1220 model, *Biogeosciences*, 18, 4005–4020, <https://doi.org/10.5194/bg-18-4005-2021>, 2021.

1221 MacGillivray, C.W., Grime, J.P., and The Integrated Screening Programme, T.: Testing  
1222 Predictions of the Resistance and Resilience of Vegetation Subjected to Extreme Events,  
1223 *Funct. Ecol.*, 9, 640-649, 1995.

1224 Markewitz, D., Devine, S., Davidson, E.A., Brando, P., and Nepstad, D.C.: Soil moisture  
1225 depletion under simulated drought in the Amazon: impacts on deep root uptake, *New*  
1226 *Phytol.*, 187, 592-607, 2010.

1227 Matusick, G., Ruthrof, K.X., Brouwers, N.C., Dell, B., and Hardy, G.S.J.: Sudden forest canopy  
1228 collapse corresponding with extreme drought and heat in a mediterranean-type eucalypt  
1229 forest in southwestern Australia, *European J. Forest Res.*, 132, 497-510, 2013.

1230 Matusick, G., Ruthrof, K.X., Fontaine, J.B., and Hardy, G.E.S.J.: Eucalyptus forest shows low  
1231 structural resistance and resilience to climate change-type drought, *J. Vegetation Science*,  
1232 27, 493-503, 2016.

1233 McCarthy, M.C., and Enquist, B.J.: Consistency between an allometric approach and optimal  
1234 partitioning theory in global patterns of plant biomass allocation, *Funct. Ecol.*, 21, 713-720,  
1235 2007.

1236 McDowell, N., Pockman, W.T., Allen, C.D., Breshears, D.D., Cobb, N., Kolb, T. et al.:  
1237 Mechanisms of plant survival and mortality during drought: why do some plants survive  
1238 while others succumb to drought? *New Phytol.*, 178, 719-739, 2008.

1239 McDowell, N.G., Adams, H.D., Bailey, J.D., Hess, M., and Kolb, T.E.: Homeostatic Maintenance  
1240 Of Ponderosa Pine Gas Exchange In Response To Stand Density Changes, *Ecological*  
1241 *Applications*, 16, 1164-1182, 2006.

1242 McDowell, N.G., and Allen, C.D.: Darcy's law predicts widespread forest mortality under climate  
1243 warming, *Nature Climate Change*, 5, 669-672, 2015.

1244 McDowell, N.G., Beerling, D.J., Breshears, D.D., Fisher, R.A., Raffa, K.F., and Stitt, M.: The  
1245 interdependence of mechanisms underlying climate-driven vegetation mortality, *Trends in*  
1246 *Ecol. & Evolution*, 26, 523-532, 2011.

1247 McDowell, N.G., Fisher, R.A., Xu, C., Domec, J.C., Hölttä, T., Mackay, D.S. et al.: Evaluating  
1248 theories of drought-induced vegetation mortality using a multimodel–experiment  
1249 framework, *New Phytol.*, 200, 304-321, 2013.

1250 Medlyn, B.E., De Kauwe, M.G., Zaehle, S., Walker, A.P., Duursma, R.A., Luus, K., Mishurov,  
1251 M., Pak, B., Smith, B., Wang, Y.-P., Yang, X., Crous, K.Y., Drake, J.E., Gimeno, T.E.,  
1252 Macdonald, C.A., Norby, R.J., Power, S.A., Tjoelker, M.G. and Ellsworth, D.S.: Using  
1253 models to guide field experiments: a priori predictions for the CO<sub>2</sub> response of a nutrient-  
1254 and water-limited native Eucalypt woodland, *Glob. Change Biol.*, 22, 2834-2851, 2016.

1255 Medvigy, D., Wang, G., Zhu, Q., Riley, W.J., Trierweiler, A.M., Waring, B., Xu, X. and Powers,  
1256 J.S.: Observed variation in soil properties can drive large variation in modelled forest  
1257 functioning and composition during tropical forest secondary succession, *New Phytol*, 223,  
1258 1820-1833, <https://doi.org/10.1111/nph.15848>, 2019.

1259 Medvigy, D., Clark, K.L., Skowronski, N.S., and Schäfer, K.V.R.: Simulated impacts of insect  
1260 defoliation on forest carbon dynamics, *Environ. Res. Lett.*, 7, 045703, 2012.

1261 Medvigy, D. and Moorcroft, P.R.: Predicting ecosystem dynamics at regional scales: an  
1262 evaluation of a terrestrial biosphere model for the forests of northeastern North America,  
1263 *Philosophical Transactions of the Royal Society B: Biological Sciences*, 367, 222-235,  
1264 2012.

1265 Medvigy, D., Wofsy, S., Munger, J., Hollinger, D. and Moorcroft, P.: Mechanistic scaling of  
1266 ecosystem function and dynamics in space and time: Ecosystem Demography model version  
1267 2, *J. Geophys. Res. Biogeosciences*, 114, 2009.

1268 Mencuccini, M., Manzoni, S., and Christoffersen, B.: Modelling water fluxes in plants: from  
1269 tissues to biosphere, *New Phytol.*, 222, 1207-1222, <https://doi.org/10.1111/nph.15681>, 2019.

1270 Meir, P., Wood, T.E., Galbraith, D.R., Brando, P.M., Da Costa, A.C.L., Rowland, L. et al.:  
1271 Threshold Responses to Soil Moisture Deficit by Trees and Soil in Tropical Rain Forests:  
1272 Insights from Field Experiments, *BioScience*, 65, 882-892, 2015.

1273 Montané, F., Fox, A.M., Arellano, A.F., MacBean, N., Alexander, M.R., Dye, A. et al.:  
1274 Evaluating the effect of alternative carbon allocation schemes in a land surface model  
1275 (CLM4.5) on carbon fluxes, pools, and turnover in temperate forests, *Geosci. Model Dev.*,  
1276 10, 3499-3517, 2017.

1277 Muldavin, E.H., Moore, D.I., Collins, S.L., Wetherill, K.R., and Lightfoot, D.C.: Aboveground  
1278 net primary production dynamics in a northern Chihuahuan Desert ecosystem, *Oecologia*,  
1279 155, 123-132, 2008.

1280 Myers, J.A., and Kitajima, K.: Carbohydrate storage enhances seedling shade and stress tolerance  
1281 in a neotropical forest, *J. Ecology*, 95, 383-395, 2007.

1282 Niklas, K. J.: The scaling of plant height: A comparison among major plant clades and anatomical  
1283 grades, *Annals of Botany*, 72, 165–172, <https://doi.org/10.1006/anbo.1993.1095>, 1993.

1284 Norby, R.J., DeLucia, E.H., Gielen, B., Calfapietra, C., Giardina, C.P., King, J.S. et al.: Forest  
1285 response to elevated CO<sub>2</sub> is conserved across a broad range of productivity, *PNAS*, 102,  
1286 18052-18056, 2005.

1287 O'Brien, M.J., Leuzinger, S., Philipson, C.D., Tay, J., and Hector, A.: Drought survival of  
1288 tropical tree seedlings enhanced by non-structural carbohydrate levels, *Nature Climate  
1289 Change*, 4, 710, 2014.

1290 Obermeier, W.A., Lehnert, L.W., Kammann, C.I., Müller, C., Grünhage, L., Luterbacher, J. et al.:  
1291 Reduced CO<sub>2</sub> fertilization effect in temperate C<sub>3</sub> grasslands under more extreme weather  
1292 conditions, *Nature Climate Change*, 7, 137, 2016.

1293 Palace, M., Keller, M., and Silva, H.: NECROMASS PRODUCTION: STUDIES IN  
1294 UNDISTURBED AND LOGGED AMAZON FORESTS, *Ecological Applications*, 18, 873-  
1295 884, 2008.

1296 Petit, G., Anfodillo, T., Mencuccini, M.: Tapering of xylem conduits and hydraulic limitations in  
1297 sycamore (*Acer pseudoplatanus*) trees, *New Phytol.*, 177, 653-  
1298 664. <https://doi.org/10.1111/j.1469-8137.2007.02291.x>, 2008.

1299 Phillips, O.L., Aragão, L.E.O.C., Lewis, S.L., Fisher, J.B., Lloyd, J., López-González, G. et al.:  
1300 Drought Sensitivity of the Amazon Rainforest, *Science*, 323, 1344-1347, 2009.

1301 Phillips, O.L., van der Heijden, G., Lewis, S.L., López-González, G., Aragão, L.E.O.C., Lloyd, J.  
1302 et al.: Drought–mortality relationships for tropical forests, *New Phytol.*, 187, 631-646, 2010.

1303 Pilon, C.E., Côté, B., and Fyles, J.W.: Effect of an artificially induced drought on leaf peroxidase  
1304 activity, mineral nutrition and growth of sugar maple, *Plant and Soil*, 179, 151-158, 1996.

1305 Potter, C., Klooster, S., Hiatt, C., Genovese, V., and Castilla-Rubio, J.C.: Changes in the carbon  
1306 cycle of Amazon ecosystems during the 2010 drought, *Environ. Res. Lett.*, 6, 034024, 2011.

1307 Powell, T.L., Galbraith, D.R., Christoffersen, B.O., Harper, A., Imbuzeiro, H.M.A., Rowland, L.  
1308 et al.: Confronting model predictions of carbon fluxes with measurements of Amazon  
1309 forests subjected to experimental drought, *New Phytol.*, 200, 350-365, 2013.

- 1310 Powell, T.L., Koven, C.D., Johnson, D.J., Faybishenko, B., Fisher, R.A., Knox, Ryan G. et al.:  
 1311 Variation in hydroclimate sustains tropical forest biomass and promotes functional diversity,  
 1312 *New Phytol.*, 219, 932-946, 2018.
- 1313 Powers, J.S., Becknell, J.M., Irving, J., and Pérez-Aviles, D.: Diversity and structure of  
 1314 regenerating tropical dry forests in Costa Rica: Geographic patterns and environmental  
 1315 drivers, *Forest Ecol. Manag.*, 258, 959-970, 2009.
- 1316 Powers, J.S., and Pérez-Aviles, D.: Edaphic Factors are a More Important Control on Surface  
 1317 Fine Roots than Stand Age in Secondary Tropical Dry Forests, *Biotropica*, 45, 1-9, 2013.
- 1318 Powers, JS, Vargas G., G, Brodribb, TJ, et al.: A catastrophic tropical drought kills hydraulically  
 1319 vulnerable tree species, *Glob. Change Biol.* 2020; 26: 3122– 3133,  
 1320 <https://doi.org/10.1111/gcb.15037>, 2020.
- 1321 Pugh, T.A.M., Rademacher, T., Shafer, S. L., Steinkamp, J., Barichivich, J., Beckage, B. et al.:  
 1322 Understanding the uncertainty in global forest carbon turnover, *Biogeosciences*, 17, 3961–  
 1323 3989, <https://doi.org/10.5194/bg-17-3961-2020>, 2020.
- 1324 Rapparini, F., and Peñuelas, J.: Mycorrhizal Fungi to Alleviate Drought Stress on Plant Growth.  
 1325 In: *Use of Microbes for the Alleviation of Soil Stresses*, Volume 1 (ed. Miransari, M),  
 1326 Springer New York New York, NY, pp. 21-42, 2014.
- 1327 Reich, P.B., Hobbie, S.E., and Lee, T.D.: Plant growth enhancement by elevated CO<sub>2</sub> eliminated  
 1328 by joint water and nitrogen limitation, *Nature Geoscience*, 7, 920, 2014.
- 1329 Reich, P.B., Wright, I.J., and Lusk, C.H.: PREDICTING LEAF PHYSIOLOGY FROM SIMPLE  
 1330 PLANT AND CLIMATE ATTRIBUTES: A GLOBAL GLOPNET ANALYSIS, *Ecological*  
 1331 *Applications*, 17, 1982-1988, 2007.
- 1332 Reichstein, M., Bahn, M., Ciais, P., Frank, D., Mahecha, M.D., Seneviratne, S.I. et al.: Climate  
 1333 extremes and the carbon cycle, *Nature*, 500, 287-295, 2013.
- 1334 Reyes, J.J., Tague, C.L., Evans, R.D., and Adam, J.C.: Assessing the Impact of Parameter  
 1335 Uncertainty on Modeling Grass Biomass Using a Hybrid Carbon Allocation Strategy, 9,  
 1336 2968-2992, 2017.
- 1337 Richardson, A.D., Carbone, M.S., Keenan, T.F., Czimczik, C.I., Hollinger, D.Y., Murakami, P. et  
 1338 al.: Seasonal dynamics and age of stemwood nonstructural carbohydrates in temperate forest  
 1339 trees, *New Phytol.*, 197, 850-861, 2013.
- 1340 Rowland, L., da Costa, A.C.L., Galbraith, D.R., Oliveira, R.S., Binks, O.J., Oliveira, A.A.R. et  
 1341 al.: Death from drought in tropical forests is triggered by hydraulics not carbon starvation,  
 1342 *Nature*, 528, 119, 2015.
- 1343 Roy, J., Picon-Cochard, C., Augusti, A., Benot, M.-L., Thiery, L., Darsonville, O. et al.: Elevated  
 1344 CO<sub>2</sub> maintains grassland net carbon uptake under a future heat and drought extreme, *PNAS*,  
 1345 113, 6224-6229, 2016.
- 1346 Ruppert, J.C., Harmony, K., Henkin, Z., Snyman, H.A., Sternberg, M., Willms, W. et al.:  
 1347 Quantifying drylands' drought resistance and recovery: the importance of drought intensity,  
 1348 dominant life history and grazing regime, *Glob. Change Biol.*, 21, 1258-1270, 2015.
- 1349 Rustad, L.E.: The response of terrestrial ecosystems to global climate change: Towards an  
 1350 integrated approach, *Science of The Total Environ.*, 404, 222-235, 2008.
- 1351 Ruthrof, K.X., Breshears, D.D., Fontaine, J.B., Froend, R.H., Matusick, G., Kala, J. et al.:  
 1352 Subcontinental heat wave triggers terrestrial and marine, multi-taxa responses, *Scientific*  
 1353 *Reports*, 8, 13094, 2018.
- 1354 Scheiter, S., Langan, L., and Higgins, S.I.: Next-generation dynamic global vegetation models:  
 1355 learning from community ecology, *New Phytol.*, 198, 957-969, 2013.

- 1356 Schenk, H.J., and Jackson, R.B.: Mapping the global distribution of deep roots in relation to  
1357 climate and soil characteristics, *Geoderma*, 126, 129-140, 2005.
- 1358 Schwalm, C.R., Anderegg, W.R.L., Michalak, A.M., Fisher, J.B., Biondi, F., Koch, G. et al.:  
1359 Global patterns of drought recovery, *Nature*, 548, 202, 2017.
- 1360 Seneviratne, S.I., X. Zhang, M. Adnan, W. Badi, C. Dereczynski, A. Di Luca, S. Ghosh, I.  
1361 Iskandar, J. Kossin, S. Lewis, F. Otto, I. Pinto, M. Satoh, S.M. Vicente-Serrano, M. Wehner,  
1362 and B. Zhou, 2021: Weather and Climate Extreme Events in a Changing Climate. In  
1363 *Climate Change 2021: The Physical Science Basis. Contribution of Working Group I to the*  
1364 *Sixth Assessment Report of the Intergovernmental Panel on Climate Change* [Masson-  
1365 Delmotte, V., P. Zhai, A. Pirani, S.L. Connors, C. Péan, S. Berger, N. Caud, Y. Chen, L.  
1366 Goldfarb, M.I. Gomis, M. Huang, K. Leitzell, E. Lonnoy, J.B.R. Matthews, T.K. Maycock,  
1367 T. Waterfield, O. Yelekçi, R. Yu, and B. Zhou (eds.)], Cambridge University Press,  
1368 Cambridge, United Kingdom and New York, NY, USA, pp. 1513–1766,  
1369 doi:10.1017/9781009157896.013, 2021.
- 1370 Settele, J., Scholes, R., Betts, R., Bunn, S.E., Leadley, P., Nepstad, D., Overpeck, J.T., and  
1371 Taboada, M.A.: Terrestrial and inland water systems. In: *Climate Change 2014: Impacts,*  
1372 *Adaptation, and Vulnerability. Part A: Global and Sectoral Aspects. Contribution of*  
1373 *Working Group II to the Fifth Assessment Report of the Intergovernmental Panel on*  
1374 *Climate Change*, Cambridge University Press Cambridge, United Kingdom and New York,  
1375 NY, USA, pp. 271-359, 2014.
- 1376 Sheffield, J., Goteti, G., and Wood, E.F.: Development of a 50-Year High-Resolution Global  
1377 Dataset of Meteorological Forcings for Land Surface Modeling, *J. Climate*, 19, 3088-3111,  
1378 2006.
- 1379 Shiels, A.B., Zimmerman, J.K., García-Montiel, D.C., Jonckheere, I., Holm, J., Horton, D. et al.:  
1380 Plant responses to simulated hurricane impacts in a subtropical wet forest, Puerto Rico, *J.*  
1381 *Ecology*, 98, 659-673, 2010.
- 1382 Silva, M., Matheny, A. M., Pauwels, V. R. N., Triadis, D., Missik, J. E., Bohrer, G., and Daly, E.:  
1383 Tree hydrodynamic modelling of the soil–plant–atmosphere continuum using FETCH3,  
1384 *Geosci. Model Dev.*, 15, 2619–2634, <https://doi.org/10.5194/gmd-15-2619-2022>, 2022.
- 1385 Sippel, S., Zscheischler, J., and Reichstein, M.: Ecosystem impacts of climate extremes crucially  
1386 depend on the timing, *PNAS*, 113, 5768-5770, 2016.
- 1387 Sitch, S., HUNTINGFORD, C., GEDNEY, N., LEVY, P.E., LOMAS, M., PIAO, S.L. et al.:  
1388 Evaluation of the terrestrial carbon cycle, future plant geography and climate-carbon cycle  
1389 feedbacks using five Dynamic Global Vegetation Models (DGVMs), *Glob. Change Biol.*,  
1390 14, 2015-2039, 2008.
- 1391 Skelton, R.P., West, A.G., and Dawson, T.E.: Predicting plant vulnerability to drought in  
1392 biodiverse regions using functional traits, *PNAS*, 112, 5744-5749, 2015.
- 1393 Smith, B., Prentice, I.C., and Sykes, M.T.: Representation of vegetation dynamics in the  
1394 modelling of terrestrial ecosystems: comparing two contrasting approaches within European  
1395 climate space, *Global Ecol. Biogeo.*, 10, 621-637, 2001.
- 1396 Smith, B., Wårlind, D., Arneth, A., Hickler, T., Leadley, P., Siltberg, J. et al.: Implications of  
1397 incorporating N cycling and N limitations on primary production in an individual-based  
1398 dynamic vegetation model, *Biogeosciences*, 11, 2027-2054, 2014.
- 1399 Spasojevic, M.J., Bahlai, C.A., Bradley, B.A., Butterfield, B.J., Tuanmu, M.-N., Sistla, S. et al.:  
1400 Scaling up the diversity–resilience relationship with trait databases and remote sensing data:  
1401 the recovery of productivity after wildfire, *Glob. Change Biol.*, 22, 1421-1432, 2016.



- 1402 Sperry, J.S., Hacke, U.G., Oren, R., and Comstock, J.P.: Water deficits and hydraulic limits to  
1403 leaf water supply, *Plant, Cell & Environ.*, 25, 251-263, 2002.
- 1404 Sperry, J.S., and Love, D.M.: What plant hydraulics can tell us about responses to climate-change  
1405 droughts, *New Phytol.*, 207, 14-27, 2015.
- 1406 Sperry, J.S., Wang, Y., Wolfe, B.T., Mackay, D.S., Anderegg, W.R.L., McDowell, N.G. et al.:  
1407 Pragmatic hydraulic theory predicts stomatal responses to climatic water deficits, *New*  
1408 *Phytol.*, 212, 577-589, 2016.
- 1409 Stovall, A.E.L., Shugart, H., and Yang, X.: Tree height explains mortality risk during an intense  
1410 drought, *Nature Communications*, 10, 4385, 2019.
- 1411 Tague, C.L., and Moritz, M.A.: Plant Accessible Water Storage Capacity and Tree-Scale Root  
1412 Interactions Determine How Forest Density Reductions Alter Forest Water Use and  
1413 Productivity, *Front. Forests and Global Change*, 2, 2019.
- 1414 Tomasella M, Petrusa E, Petruzzellis F, Nardini A, Casolo V.: The Possible Role of Non-  
1415 Structural Carbohydrates in the Regulation of Tree Hydraulics, *International Journal of*  
1416 *Molecular Sciences*, 21:144, <https://doi.org/10.3390/ijms21010144>, 2020.
- 1417 Trugman, A.T., Detto, M., Bartlett, M.K., Medvigy, D., Anderegg, W.R.L., Schwalm, C. et al.:  
1418 Tree carbon allocation explains forest drought-kill and recovery patterns, *Ecol. Lett.*, 21,  
1419 1552-1560, 2018.
- 1420 Trugman, A.T., Anderegg, L.D.L., Sperry, J.S., Wang, Y., Venturas, M., Anderegg,  
1421 W.R.L.: Leveraging plant hydraulics to yield predictive and dynamic plant leaf allocation in  
1422 vegetation models with climate change, *Glob. Change*  
1423 *Biol.*, 25, 4008– 4021. <https://doi.org/10.1111/gcb.14814>, 2019.
- 1424 Uriarte, M., Lasky, J.R., Boukili, V.K., and Chazdon, R.L.: A trait-mediated, neighbourhood  
1425 approach to quantify climate impacts on successional dynamics of tropical rainforests,  
1426 *Funct. Ecol.*, 30, 157-167, 2016.
- 1427 Vargas G., G., Brodribb, T.J., Dupuy, J.M., González-M., R., Hulshof, C.M., Medvigy, D.,  
1428 Allerton, T.A.P., Pizano, C., Salgado-Negret, B., Schwartz, N.B., Van Bloem, S.J., Waring,  
1429 B.G. and Powers, J.S.: Beyond leaf habit: generalities in plant function across 97 tropical  
1430 dry forest tree species, *New Phytol*, 232: 148-161. <https://doi.org/10.1111/nph.17584>, 2021.
- 1431 Venturas, M. D., Todd, H. N., Trugman, A. T., and Anderegg, W. R.: Understanding and  
1432 predicting forest mortality in the western United States using long-term forest inventory data  
1433 and modeled hydraulic damage, *New Phytol.*, 230, 1896-1910, 2021.
- 1434 Wang, D., Heckathorn, S.A., Wang, X., and Philpott, S.M.: A meta-analysis of plant  
1435 physiological and growth responses to temperature and elevated CO<sub>2</sub>, *Oecologia*, 169, 1-13,  
1436 2012.
- 1437 Weng, E.S., Malyshev, S., Lichstein, J.W., Farrior, C.E., Dybzinski, R., Zhang, T. et al.: Scaling  
1438 from individual trees to forests in an Earth system modeling framework using a  
1439 mathematically tractable model of height-structured competition, *Biogeosciences*, 12, 2655-  
1440 2694, 2015.
- 1441 Williams, A.P., Allen, C.D., Macalady, A.K., Griffin, D., Woodhouse, C.A., Meko, D.M. et al.:  
1442 Temperature as a potent driver of regional forest drought stress and tree mortality, *Nature*  
1443 *Climate Change*, 3, 292, 2012.
- 1444 Williams, A.P., Seager, R., Berkelhammer, M., Macalady, A.K., Crimmins, M.A., Swetnam,  
1445 T.W. et al.: Causes and Implications of Extreme Atmospheric Moisture Demand during the  
1446 Record-Breaking 2011 Wildfire Season in the Southwestern United States, *J. Applied*  
1447 *Meteorology and Climatology*, 53, 2671-2684, 2014.

- 1448 Williams, L.J., Bunyavejchewin, S., and Baker, P.J.: Deciduousness in a seasonal tropical forest  
1449 in western Thailand: interannual and intraspecific variation in timing, duration and  
1450 environmental cues, *Oecologia*, 155, 571-582, 2008.
- 1451 Wullschleger, S.D., Hanson, P.J., and Todd, D.E.: Transpiration from a multi-species deciduous  
1452 forest as estimated by xylem sap flow techniques, *For. Ecol. and Manage.*, 143, 205-213,  
1453 2001.
- 1454 Xu, X., Medvigy, D., Powers, J.S., Becknell, J.M. and Guan, K.: Diversity in plant hydraulic  
1455 traits explains seasonal and inter-annual variations of vegetation dynamics in seasonally dry  
1456 tropical forests, *New Phytol.*, 212, 80-95, 2016.
- 1457 Yang, Y., Hillebrand, H., Lagisz, M., Cleasby, I., and Nakagawa, S.: Low statistical power and  
1458 overestimated anthropogenic impacts, exacerbated by publication bias, dominate field  
1459 studies in global change biology. *Glob. Change Biol.*, 28, 969– 989,  
1460 <https://doi.org/10.1111/gcb.15972>, 2022.
- 1461 Zhu, K., Chiariello, N.R., Tobeck, T., Fukami, T., and Field, C.B.: Nonlinear, interacting  
1462 responses to climate limit grassland production under global change, *PNAS*, 113, 10589-  
1463 10594, 2016.
- 1464 Zhu, S-D., Chen, Y-J., Ye, Q., He, P-C., Liu, H., and Li, R-H., et al.: Leaf turgor loss point is  
1465 correlated with drought tolerance and leaf carbon economics traits, *Tree Physiol.*, 38, 658–  
1466 663, <https://doi.org/10.1093/treephys/tpy013>, 2018.
- 1467 Zscheischler, J., Mahecha, M.D., von Buttlar, J., Harmeling, S., Jung, M., Rammig, A. et al.: A  
1468 few extreme events dominate global interannual variability in gross primary production,  
1469 *Environ. Res. Lett.*, 9, 035001, 2014.